CHALMERS
UNIVERSITY OF TECHNOLOGY

Lithium-Ion Battery Storage for Frequency Control

Tentative Implementation in the Nordic Power System

Master's thesis in Electric Power Engineering

LUCAS THOMÉE

Department of Electrical Engineering
CHALMERS UNIVERSITY OF TECHNOLOGY
Gothenburg, Sweden 2018

Lithium-Ion Battery Storage for Frequency Control

Tentative Implementation in the Nordic Power System

CHALMERS
UNIVERSITY OF TECHNOLOGY

Department of Electrical Engineering
Division of Electric Power Engineering
CHALMERS UNIVERSITY OF TECHNOLOGY
Gothenburg, Sweden 2018

Lithium-Ion Battery Storage for Frequency Control
Tentative Implementation in the Nordic Power System
LUCAS THOMÉE

© LUCAS THOMÉE, 2018.

Supervisor: Lena Max, DNV-GL
Examiner and supervisor: Jimmy Ehnberg, Department of Electrical Engineering

Master's Thesis 2018
Division of Electric Power Engineering
Department of Electrical Engineering
Chalmers University of Technology
SE-412 96 Gothenburg
Sweden
Telephone +46 31 772 10 00

Typeset in LaTeX
Gothenburg, Sweden 2018

Lithium-Ion Battery Storage for Frequency Control
Tentative Implementation in the Nordic Power System
LUCAS THOMÉE
Department of Electrical Engineering
Chalmers University of Technology

Abstract

With increased integration of converter connected production, decommission of nuclear power plants in Sweden, reduction in frequency dependent loads, and increased import through HVDC links, the power system frequency stability in the Nordic power system is at risk. Reduced system frequency stability caused by the reduction of inertia, affects reliability and quality and could result in increased frequency deviation and possibly power outages. New services contributing to frequency stability are needed.

This thesis investigates the possibilities of using battery energy storage systems in Sweden, a part of the Nordic synchronous power system, to provide frequency control. This is done by determining the role inertia has and how frequency is regulated in the Nordic power system. The battery storage system development is evaluated and different battery technologies are assessed. A dynamic model of the Nordic power system and two control models for lithium-ion battery storage systems are developed in PSS/E. These models are then combined and simulations of frequency deviations are performed.

The results indicate that large lithium-ion battery storage system controlled to provide inertial response reduce rate of change of frequency, reduce the maximum instantaneous frequency deviation, and delay time to frequency nadir. With droop controlled battery storage systems providing FCR-D, the reduction in maximum instantaneous frequency deviation is significant. It is found that using a single derivative controlled 540 MW unit results in frequency distortion, while using a droop controlled unit of the same size does not cause any frequency distortion. It is also confirmed that 540 MW derivative controlled battery storage systems can provide the equivalent of 130 000 MWs kinetic energy for the reference case.

The feasibility study illustrates the difficulty in finding economic incentives when lithium-ion battery storage systems are used to provide FCR-D. Current regulations and markets in Sweden and the Nordic power system do not enable the deployment of lithium-ion for this application, despite its indicated benefits. The recommendation is to create new markets and investigate additional services for battery applications in the Nordic synchronous power system.

Keywords: Inertial response, primary frequency regulation, battery energy storage systems, frequency reserve, Nordic synchronous power system.

Acknowledgements

My profound gratitude and thanks goes to Lena Max, my supervisor at DNV GL, for her guidance and support throughout my work. I would also like to thank everyone else in the PSA department and everyone in the Gothenburg office for their help whenever I have had any questions and for creating such a welcoming and inspiring workplace. Special thanks goes to my friends and those closest to me for being there during my ups and downs, without you this would not have been possible.

Lucas Thomée, Gothenburg, May 2018

Contents

List of Figures

1
Introduction

Renewable energy generation is increasingly integrated in power systems all over the world to create a cleaner generation capacity and reduce reliance on fossil fuels. However, increased integration of renewable energy sources and reduction in conventional power generation creates issues in the power system. One potential problem is the decrease in power system kinetic energy, also known as inertia, resulting in reduced system frequency stability. This could severely affect system reliability, safety and quality. To maintain high operational reliability, new services for frequency control and alternative sources providing the equivalent to inertia and kinetic energy should be investigated.

This master's thesis work investigates the possibilities of using battery energy storage systems for inertial response and frequency regulation in Sweden as a part of the Nordic synchronous power system. This is done by exploring the currently available battery and converter technologies and their suitability for frequency regulation and in providing inertial response. The proposed solution is modeled and simulated in a model of the Swedish power system in PSS/E to illustrate the usefulness of the technology.

1.1 Background

In Sweden, nuclear power plants are being decommissioned, power generation is moving towards increased integration of distributed energy sources, such as solar and wind, and at the same time there is a reduction in frequency dependent loads and increase in import through HVDC links [1], [2]. This is expected to have a large impact on system reliability [1], [2]. At the same time, society has a growing dependence on a reliable, secure and high quality supply of electricity [1], [2]. The Swedish transmission system operator is responsible to provide the means and maintain the conditions required to supply high quality electricity. Part of supplying high quality electricity is the ability to maintain the frequency in the power system at nominal levels by regulating changes in production and consumption, and manage disturbances [1]-[3].

Inertia in a power system context is the result of naturally occurring kinetic energy stored in rotating synchronous generators [2], [3]. The amount of kinetic energy available depends on the type of energy source used. In Sweden, as a part of the Nordic system, there has traditionally been an abundant amount of kinetic energy

from hydro generators, nuclear and other thermal power plants [1], [2]. With changes happening in Sweden, inertia is decreased [1], [2], [4].

Inertia reduces the rate of change of frequency caused by imbalances in production and consumption, allowing output of generators to be adjusted and therefore contributes to the power system's ability in reducing frequency deviations [2], [3]. Reduced inertia results in an increased risk of large power outages following a severe system event [1]-[3]. A frequency event could be a large power deficit after a generation unit is disconnected or a large sudden deficit in load. There is therefore a need to consider solutions related to the future shortage of inertia in the power system.

One possible solution would be to improve power system equipment and protection systems to cope with faster and larger frequency deviations, and change the technical requirements set by the grid code standards to allow the power system to run at lower levels of inertia [1]-[3]. Another option would be to try and regulate frequency by other means or provide synthetic inertia from alternative sources. This could be realized by converter connected production, synchronous condensers or battery energy storage systems [1]-[4].

Battery energy storage systems are deemed to be a viable option in providing frequency response because they can quickly and precisely regulate the power output to the power system [4]-[7]. This study therefore investigates the issue of future inertia deficiency, available battery technologies and the role battery storage could play in power system frequency control.

1.2 Aim

To investigate the possibility of providing inertial response and frequency regulation in the Nordic synchronous power system using battery energy storage systems in Sweden.

1.3 Problem

First there is a need to understand and present the impact inertia has on the power system and how frequency is regulated in the Nordic synchronous system. Following the recent development of battery storage, the possibilities to utilize the technology to provide the power system with frequency response are reviewed. This is to determine the important characteristics of current battery systems and converters available.

Another part of the work is to illustrate the possibility of using battery energy storage systems in regulating frequency and the resulting effects, using a dynamic model of the Nordic power system. Modeling and subsequent simulations are done in PSS/E. It is first required to verify that the model of the grid resembles the

actual system and fulfills the requirements during dynamic simulation. Models of the dynamic characteristics of the battery storage system need to be created to execute simulations showing how the frequency regulation is handled by battery energy storage systems in comparison to the conventional regulators.

The result illustrates the usefulness of the technology and is explained and presented in a way that it can be used to educate people interested in the subject, i.e. the Swedish TSO and actors in the frequency reserve market. An ongoing part of the study is therefore presenting, summarizing and discussing the findings and results in a way that the work can be understood and used for further studies. Additional tasks include looking at the placement of the technology in the grid and additional possible power system applications, other than inertial response and primary frequency regulation.

It is assessed that this study needs to consider sustainable and ethical aspects of the project. The environmental effects of production and intended use of batteries in the power system, and the possible ethical and societal consequences of using batteries in the power system, mainly focused on the current working conditions during the mining of material and production of batteries, are covered. Batteries in the power system is also compared to the alternatives, which are continued used of convectional generation or providing services from other technologies. The ethical discussion also reflects on how the thesis work is carried out.

1.4 Scope

The thesis work is focused on the Nordic power system and the simulation is done in a model of the Swedish transmission grid based on open source material. The work is therefore limited to Sweden and determining if the outcome is viable or possible to adjust to requirements in other regions is not within the scope of the work.

Based on the characteristics of battery energy storage systems it is deemed that most viable power system applications are inertial response and primary frequency control [4]-[7]. Focus is therefore on regulating frequency following disturbances, which includes Inertial Response and Frequency Containment Reserve - Disturbance (FCR-D), as denoted by the European Network of Transmission System Operators for Electricity (ENTSO-E). Voltage stability is not examined in dynamic simulations.

The thesis work is limited to large battery storage systems dedicated to providing frequency regulation in large interconnected transmission systems. The battery system technologies studied are lead-acid, vanadium based flow batteries, sodium-sulfur and lithium-ion. These battery types have shown to exhibit the desired characteristics required for frequency regulation in large power systems [5], [7]-[11].

2
Method

A literature study was conducted to describe how inertia is supplied and used in frequency regulation in the Nordic synchronous power system today. The requirements on frequency stability with focus on inertial response and FCR-D were covered. This was covered to understand the need and requirements of inertial response and FCR-D and how battery energy storage systems could provide it.

A thorough description of the current state of the development of battery technologies for power system applications was then carried out through a literature review and personal contact with battery experts. This included characteristics and suitability of different battery types, controls and power electronics for providing frequency regulation in the Swedish power system. Also, a more detailed explanation of aging mechanism of lithium-ion batteries was covered. This was conducted to acquire an understanding of the battery technologies.

A static model of the Swedish power system created in PSS/E with dynamic characteristics of Nordic synchronous power system was complemented. An already developed model was used because it was based on open source to avoid any associated issues and because of simplicity reasons. It was confirmed it performed as expected by comparing the frequency response of the model to system requirements and a recorded historical reference response and load case.

The effects of reduced inertia on the system were also illustrated by reducing the level of kinetic energy in the model from initial 260 000 MWs to 130 000 MWs, and 80 000 MWs. 130 000 MWs was chosen at it is a low inertia case for the current power system, and 80 000 MWs since it is an estimated minimum for the future power system. Some minor differences between model and reality were observed, which are the result of using an aggregated model. These small deviations were deemed acceptable for this projects.

The battery type deemed most suited for the purpose was chosen based on the performance parameters: discharge cycles, energy efficiency, maturity, costs and sustainable aspects. These parameters were chosen as they are deemed the most important for the intended application. Two dynamic frequency models were then designed as user defined models for PSS/E. One based on derivative control to provide inertial response and one droop control to provide FCR-D.

Simulations using the Nordic dynamic model and battery storage models were per-

formed to see the effects on frequency following a disturbance. The simulated cases were based on a reference response case with additional 40, 100 and 540 MW battery capacities. The reference case was chosen to be a high load production hour on March 05, 2015 where Ringhals 4 was suddenly disconnected resulting in 1110 MW power deficiency. This case was chosen as it enabled verification of the model. 40 MW power capacity was chosen as there are several battery storage systems of that size installed globally. 100 MW is the power rating of the largest installed unit to date. 540 MW was chosen as it is the power corresponding to increasing kinetic energy from 130 000 MWs to 260 000 MWs.

Results from the simulated cases were then compared to each other based on performance, in terms of reducing frequency deviation magnitude, time to nadir and reduction in oscillations. These performance parameters are deemed to be the most important when discussing frequency deviations. The results were used to verify the hypothesis that batteries can provide frequency stability support. An economic and lifetime analysis was conducted to conclude where further development in the area needs to be focused.

The discussion handled the significant findings and limits of the results. The sustainable and ethical aspects of the project, introduced in section 1.3, were also considered by performing an investigation and discussion of these issues.

3

System Frequency Stability

In an AC power system, the frequency which the system is operating at is used as an indication of the balance between generation and load. If there is an imbalance frequency will deviate from its nominal value. To ensure operational security, frequency should be kept within nominal limits, which in Sweden as a part of the Nordic synchronous system is 50 ± 0.1 Hz [2], [3], [12].

Power system stability is defined as the ability to remain in operational balance following a disturbance and under normal conditions [13]. To achieve balance, production is carefully planned to meet demand, but the power system must also be able to regain balance after unexpected deviations in production and consumption [2], [12], [14]. This is realized through characteristics of the power system and using various control methods.

3.1 Inertia and Kinetic Energy

In general terms inertia is defined as the resistance of an object to any change in its speed, direction or state of rest. In a power system context, inertia is the ability to resist changes in system frequency [12]. The objects subject to a change of motion are the rotating synchronous machines and inertia is the resistance to change in rotational speed of the machines [3], [12].

When there is an imbalance between production and consumption frequency will change and the rotating speed of machines will be affected [2]. Inertia enables continuous operation of the power system by limiting rate of change of frequency and thereby assists in countering the imbalance between production and consumption to restore frequency [2], [3], [12]. Inertia is provided from rotating machines by their ability to absorb energy from the grid or inject energy into the grid using their stored kinetic energy [3].

In a simplified conventional system, assuming only synchronous connected generators and absence of frequency dependent loads, the system inertia is provided from kinetic energy stored in the rotational mass of turbines and generators [2], [3], [12].

To derive an expression for system inertia there is a need to look at the inertia of a single generator. Kinetic energy (E_k) in generator at nominal angular frequency ω_0

can be expressed as

$$E_k = \frac{I\omega_0^2}{2} \tag{3.1}$$

where I is the moment of inertia [15].

The inertia constant H_g is often expressed as kinetic energy in a generator proportional to its power rating (S_g). Resulting in

$$H_g = \frac{E_k}{S_g} = \frac{\frac{I\omega_0^2}{2}}{S_g} \tag{3.2}$$

where the inertia constant H_g is a measurement in seconds of how long the kinetic energy stored in a generator can provide nominal power [2], [3], [15]. Total system inertia (H_{sys}) can then be expressed as

$$H_{sys} = \frac{\sum E_k}{\sum S_g} = \frac{\sum E_k}{S_{sys}} \tag{3.3}$$

where S_{sys} is the total generation capacity [3], [12]. In other words, the system inertia is the sum of stored kinetic energy in generators divided by the total generation capacity as shown in equation (3.3).

In some cases, it can be more relevant to consider the system kinetic energy (E_{ksys}) expressed in megawatt seconds rather than system inertia expressed in seconds [12]. Equation (3.3) can then be written as

$$E_{ksys} = \sum H_g S_g = H_{sys} S_{sys} \ . \tag{3.4}$$

3.1.1 Swing Equation

Frequency dynamics of power systems can be explained by the swing equation. It describes the change in kinetic energy of generators in a power system, expressed as

$$\frac{dE_k}{dt} = P_g - P_l \tag{3.5}$$

where P_g is the total generated power and P_l the system load [3], [16]. It shows that an imbalance between generation and load will result in a change in kinetic energy of the rotating masses. Since kinetic energy is proportional to frequency, it will result in a change in frequency [16].

The frequency dependence of the system inertia can be derived from equations (3.3) and (3.5), and simplifying, which gives

$$\frac{2H_{sys}}{f_0}\frac{df}{dt} = \frac{P_g - P_l}{S_{sys}} \tag{3.6}$$

where f_0 is the nominal system frequency and $\frac{df_0}{dt}$ is known as the rate of change of frequency (RoCoF) [4], [15], [16].

Equation (3.6) can be rewritten as

$$\frac{df}{dt} = \frac{f_0 \Delta P}{2H_{sys}S_{sys}} = \frac{f_0 \Delta P}{2E_{ksys}} \tag{3.7}$$

describing the relation of H_{sys} and E_{ksys} to RoCoF in a system with nominal frequency f_0 for a disturbance ΔP. When an imbalance occurs, the kinetic energy works to counteract the change in frequency and with greater inertia the change in frequency is reduced. This shows how inertia helps improve frequency stability [3], [12].

3.2 Frequency Regulation in Sweden

When there is an imbalance in the power system the frequency will deviate from 50 Hz. Frequency regulation is the action of restoring balance between production and consumption in the power system. In Sweden, frequency regulation can be divided into primary, secondary and tertiary frequency regulation [17].

ENTSO-E has divided the frequency reserve needed to restore power balance into Frequency Containment Reserve (FCR) and Frequency Restoration Reserve (FRR). FCR can further be divided into Frequency Containment Reserve for Normal operation (FCR-N) and Frequency Containment Reserve for Disturbed operation (FCR-D). FRR is divided into automatic FRR (aFRR) and manual FRR (mFRR). Table 3.1 summarizes the different parts of frequency regulation and correlation to respective frequency reserve.

Table 3.1: Frequency regulation measures and corresponding frequency reserves as defined by the Swedish TSO and ENTSO-E.

Frequency Regulation	**Frequency Reserve**
Primary	FCR
Secondary	aFRR
Tertiary	mFRR

The stages of restoring frequency following an imbalance in the power system are illustrated in Figure 3.1.

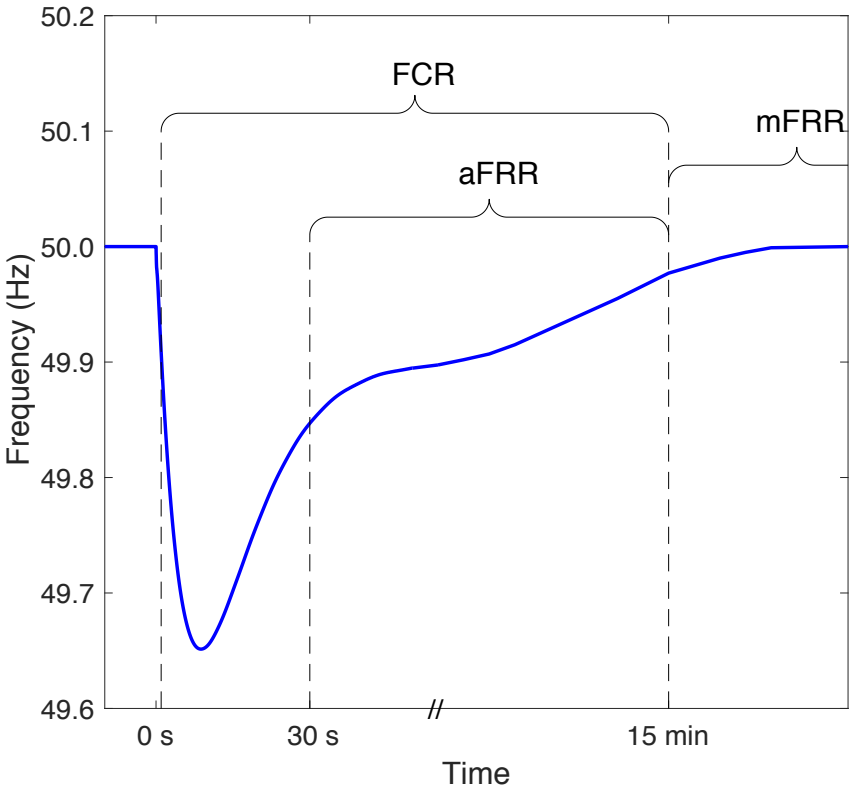

Figure 3.1: The different frequency regulation stages. The frequency event occurs at 0 seconds and shortly after primary frequency regulation with FCR is activated. Within 30, seconds secondary frequency regulation with aFRR is activated and tertiary frequency regulation with mFRR is activated after maximum 15 minutes.

As seen in Figure 3.1, primary frequency regulation with FCR starts shortly after the frequency event. This reduces the change in frequency to zero where frequency is at its lowest point. Secondary frequency regulation with aFRR is activated within 30 seconds and tertiary frequency regulation with mFRR within 15 minutes. Primary frequency regulation reestablishes steady state frequency at a lower value than nominal and the aim of the secondary and tertiary frequency regulation is to restore frequency to its nominal value.

3.2.1 Inertial Response

Before primary frequency regulation is activated there is first an inertial response. This is where the stored kinetic energy in rotating machines counters the frequency deviation. The general operation of inertial response and FCR during a frequency event is illustrated in Figure 3.2.

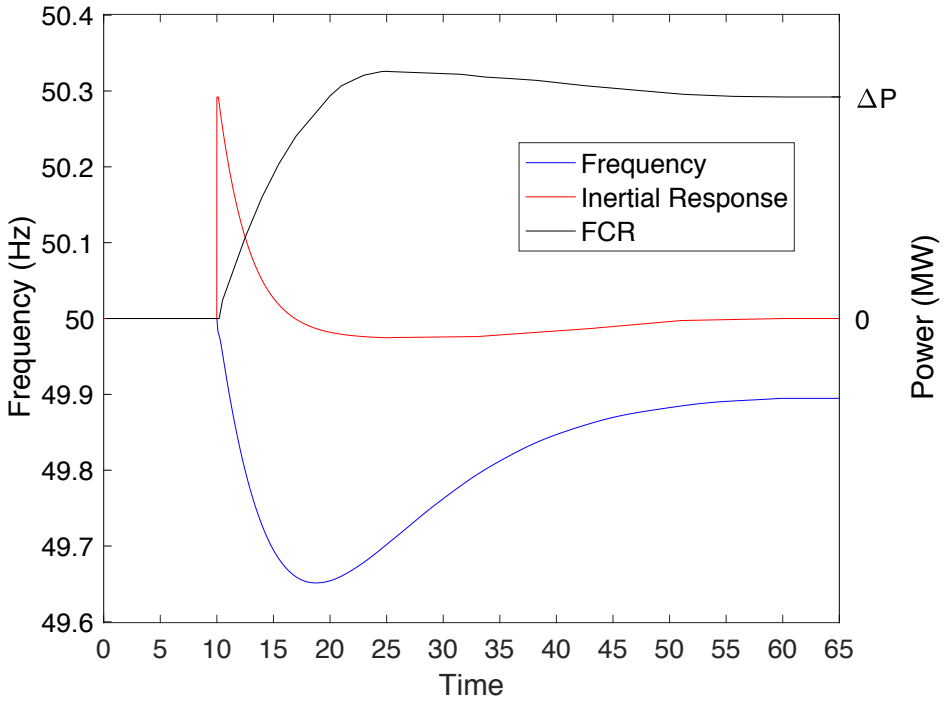

Figure 3.2: Frequency, inertial response and FCR. At the start of the frequency event at 10 seconds, inertial response replaces the loss in production ΔP. When FCR increases inertial response decreases. Frequency is reestablished at a new steady state frequency when FCR is at ΔP and inertial response at 0 MW.

As seen in Figure 3.2, at the start of the frequency event at 10 seconds inertial response is at its peak and it is gradually reduced when FCR is activated. Inertial response changes from positive to negative when maximum frequency deviation has been reached, as this is where the synchronous rotating machines start to accelerate, and is reduced to zero when steady state frequency is reached [12]. Steady state frequency is at roughly 49.9 Hz for this case and this is when FCR reaches ΔP.

As depicted in equation (3.6), RoCoF depends on system kinetic energy, and larger inertia results in greater kinetic energy and longer time to counter the power imbalance. Inertia is therefore vital for the power system to function as controllers responsible to restore frequency need time to respond [2], [3], [12].

At the moment, there is no defined minimum requirement on inertia or kinetic energy in the System Operation Agreement (SOA) in the Nordic power system [14]. There is therefore no defined limit to lowest point of frequency following a disturbance [14], [18]. However, in the Nordic power system load shedding will commence at 49.0 Hz and this level can be used as minimum acceptable transient frequency level [18].

3.2.2 Primary Frequency Regulation

Inertial response is followed by primary frequency regulation, where both FCR-N and FCR-D are active. During normal operation, when frequency is in the range of 50 Hz ± 0.1 Hz, FCR-N is used to control frequency. The procedure using FCR-N is automatically activated by frequency deviations from 50.0 Hz to keep the frequency within the limits 49.9 - 50.1 Hz [14], [17], [19].

In the Nordic power system 600 MW FCR-N is required and the distribution of FCR-N in each country is based on the annual consumption of the previous year [2], [17], [18]. The volume requirement for Sweden is roughly 200 MW. Technical requirements set by the Swedish TSO on FCR-N states that for a gradual change in frequency 63 % should be activated within 60 seconds, and 100 % within 3 minutes [19].

If the frequency deviates beyond 50 ± 0.1 Hz FCR-D is activated. After a major disturbance inertia prevents the frequency deviation from getting too large before FCR-D can stabilize the frequency. The objective of FCR-D is to reduce the change in frequency to zero and stabilize the frequency at a steady state value [14], [17], [19].

According to SOA, the requirement for FCR-D in the Nordic system is that it should be able to handle the fault of the largest production unit or HVDC link subtracted by 200 MW, for frequency dependent load, without resulting in steady state frequency below 49.5 Hz [14], [18]. For the dimensioning fault of 1400 MW in the Nordic system total FCR-D is 1200 MW.

The distribution of FCR-D is carried out in proportion to the dimensioning fault within the respective country, which is shown in Table 3.2.

Table 3.2: Distribution of FCR-D to Sweden, Norway, Finland and Denmark based on dimensioning fault, according to System Operation Agreement [18].

Country	**Dimensioning Fault [MW]**	**Reserve [MW]**
Sweden	1 400	412
Norway	1 200	353
Finland	880	259
Denmark	600	177
Total	4 080	1 200

Per the network code on requirements for generators in the Swedish system [20], generators are allowed a maximum of 2 second delay to regulate power output. The technical requirements declared by the Swedish TSO state that units providing FCR-D should for a gradual change in frequency activate 50 % within 5 seconds, and 100 % within 30 seconds [19]. The requirements from ENTSO-E on the Nordic system state that FCR-D must be fully restored within 15 minutes to be capable of handling a new disturbance [21], [22].

3.2.3 Secondary Frequency Regulation

After a major disturbance, secondary frequency regulation is needed in order to return frequency to the nominal value [17]. The objective of secondary frequency regulation is to restore the frequency to 50 Hz after it has stabilized at steady state frequency by primary frequency regulation [17], [23]. This is an automatic process using aFRR.

In the Nordic system, the requirement on aFRR is 300 MW of which 100 MW should be provided in the Swedish system [24]. aFRR should be automatically activated when a control signal is sent by the Swedish TSO. The requirement is that units providing aFRR have to act within 30 seconds and 100 % of aFRR should be activated within 2 minutes [19], [23].

3.2.4 Tertiary Frequency Regulation

The tertiary frequency regulation with mFRR is used to balance power and handle congestion in normal and disturbed operation. When activated it works as a replacement for FCR and aFRR to bring the frequency to 50 Hz [17], [19]. It is the main balancing resource and the requirement is that it should be activated within 15 minutes [14].

Following a frequency deviation both secondary and tertiary frequency regulation are used to replace primary frequency regulation so that FCR-N and FCR-D can be replenished. This is to allow the system to be ready for another frequency deviation within 15 minutes [22].

3.2.5 Fast Frequency Response

Currently there is a discussion of introducing another term in frequency regulation, denoted Fast Frequency Response (FFR) [7], [23], [25]. It can be defined as a reserve service provided by technologies capable of responding faster than conventional reserves to frequency deviations [23], [7]. Examples of technologies capable of delivering FFR are wind turbines, different types of energy storage systems, and HVDC links. It could also possibly be provided from demand response or vehicle-to-grid solutions [23].

Battery energy storage systems (BESS) are a potential source of FFR. Compared to traditional frequency reserves it has limited energy capacity but it possesses other benefits and characteristics capable of assisting in maintaining system frequency. Currently these are not fully recognized in defined reserve services in the Nordic power system [7]. Conventional reserves, FCR and FRR, are procured through existing frequency response markets [24]. Since FFR differs from existing reserve it is suggested to alter current definitions of services and markets or design new markets to secure the full advantages of technologies capable of providing FFR [7], [25].

In Great Britain, the TSO National Grid has created a new ancillary service market

called Enhanced Frequency Response (EFR). 201 MW is procured for new technologies capable of providing FFR with the requirement of maximum response time of 1 second [26]. This service is directly designed for battery storage as it allows the battery to charge and discharge when it is not providing its service [7]. This is just one example of how BESS are becoming competitive with traditional methods of managing frequency when their capabilities are recognized. It also shows how new services and markets need to be created to adjust to a future power system to handle potential issues.

3.3 Frequency Dependence of Generators

When the frequency in a grid deviates from its nominal value, available control reserves are automatically activated as explained in section 3.2. The change in output from generators depends on the frequency deviation and can be described by the droop constant or setting R [2]. R in % is defined as

$$R = \frac{\Delta f / f_0}{\Delta P / P_0} \cdot 100 \tag{3.8}$$

where Δf is the frequency change, f_0 nominal frequency, ΔP change in power and P_0 nominal power [2]. The droop constant describes the power to frequency characteristics of the generator speed governor setting [2], [27], illustrated in Figure 3.3.

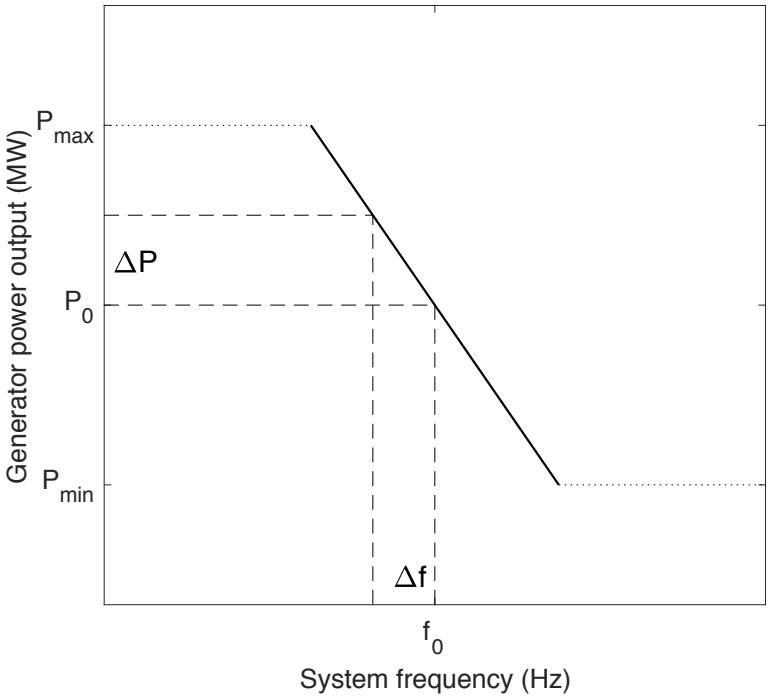

Figure 3.3: The figure illustrates the linear relationship of droop setting R, which is the slope and indicates how much generator power output changes following a change in system frequency. If frequency is reduced from nominal system frequency f_0 by Δf, power will increase by ΔP from nominal power output P_0. Generator output can be limited by P_{max} and P_{min} indicated by the dotted lines.

As shown in Figure 3.3, the droop setting R is a linear relationship between frequency deviation and power output. With a decrease in frequency the power output will increase following slope R, and when the frequency increases power output will decrease. A low droop constant results in a steeper slope and a more powerful response by the power supply [2].

The droop setting also helps explain why the frequency is not restored to its nominal value by FCR-D. As described in subsection 3.2.2, following a frequency deviation, output of generators providing reserve will adjust to compensate for the power imbalance. When power balance is restored, the power output setting of generators has changed and frequency will be stabilized at a steady state value, which is different from nominal frequency. Secondary frequency regulation is therefore needed to provide additional power allowing the primary reserves to return to their nominal power output setting to be prepared for another deviation [12], [22].

3.4 Frequency Dependence of Loads

Similar to the frequency dependence of generators, loads in the form of synchronous machines are also frequency dependent [2]. When frequency deviates the power demand will change, similar to the droop setting of generators illustrated in Figure 3.3 but with an opposite sign. If the frequency decreases demand will decrease and

if frequency increases the load will increase, which is opposite from the response of production. This is described as the self-regulating power of the system as it helps reduce power imbalance [12]. The impact of frequency regulation from loads is less than that of generators and is expected to decrease further with increased integration of converter connected loads [2].

3.5 System Frequency Response

The system frequency response or the power/frequency characteristic indicates how much the power production changes with a change in system frequency. It is denoted λ, defined as

$$\lambda = \frac{\Delta P}{\Delta f} \tag{3.9}$$

where Δf is the frequency deviation following a disturbance and λ is measured in [MW/Hz] [18, 27]. The requirements of system frequency response in the Nordic power system are illustrated in Figure 3.4.

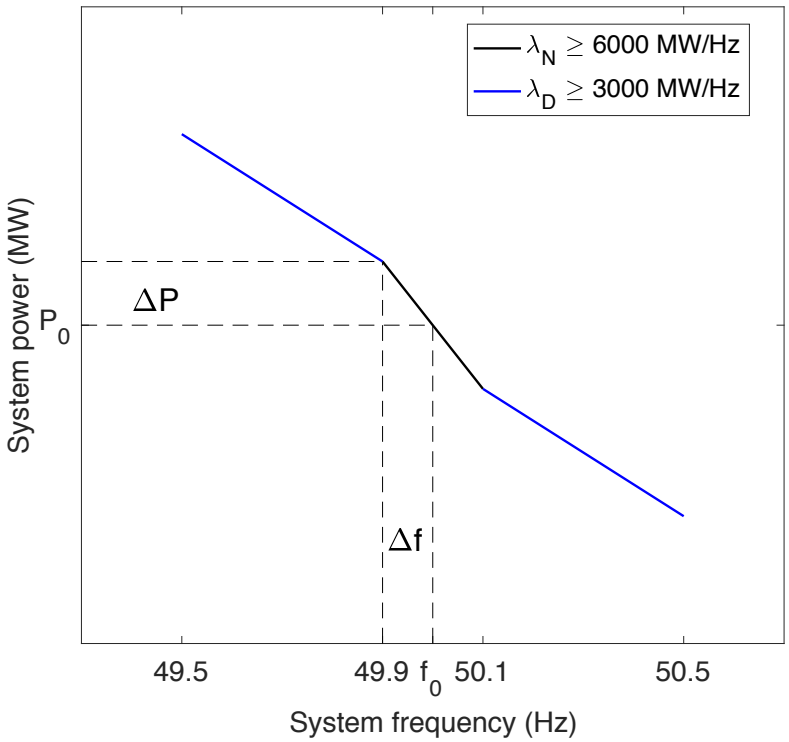

Figure 3.4: The frequency response requirements in the Nordic synchronous system. Frequency response λ is the ratio of $\frac{\Delta P}{\Delta f}$. In the normal operating region, 50 $\pm$ 0.1 Hz, the requirement λ_N on FCR-N is 6000 MW/Hz. For deviations until 49.5 and 50.5 Hz, λ_D of 3000 MW/Hz is required for FCR-D [2], [18].

As mentioned in subsection 3.2.2, the requirement in the Nordic synchronous system on FCR-N is at least 600 MW at deviations of 0.1 Hz and for FCR-D 1200 MW

at additional deviation of 0.4 Hz. As shown in Figure 3.4, the frequency regulation requirement is therefore at least 6000 MW/Hz for normal operation, within 50 ± 0.1 Hz. For disturbed operation with deviations until 49.5 or 50.5 Hz, the requirement is at least 3000 MW/Hz [18].

4

Battery Energy Storage Systems

Battery energy storage systems (BESS) have the potential to change the concept of power generation, transmission, and consumption. Further development is needed before electricity can be stored in large amounts, but technology available today can be implemented and used for several power system applications [4]-[7]. BESS have rapid response times and can precisely regulate power input and output, and therefore they are deemed a viable option in providing frequency regulation [4]-[7]. In this chapter, current BESS technologies for frequency regulation are reviewed.

Essentially a general BESS consists of a battery system, power conversion system, and battery management system. Figure 4.1 shows this configuration. The battery system is where the energy is stored. The power conversion system handles the conversion of energy from the battery to the grid, and the other way around. Lastly, the management system monitors and controls the battery and overall system [5], [28].

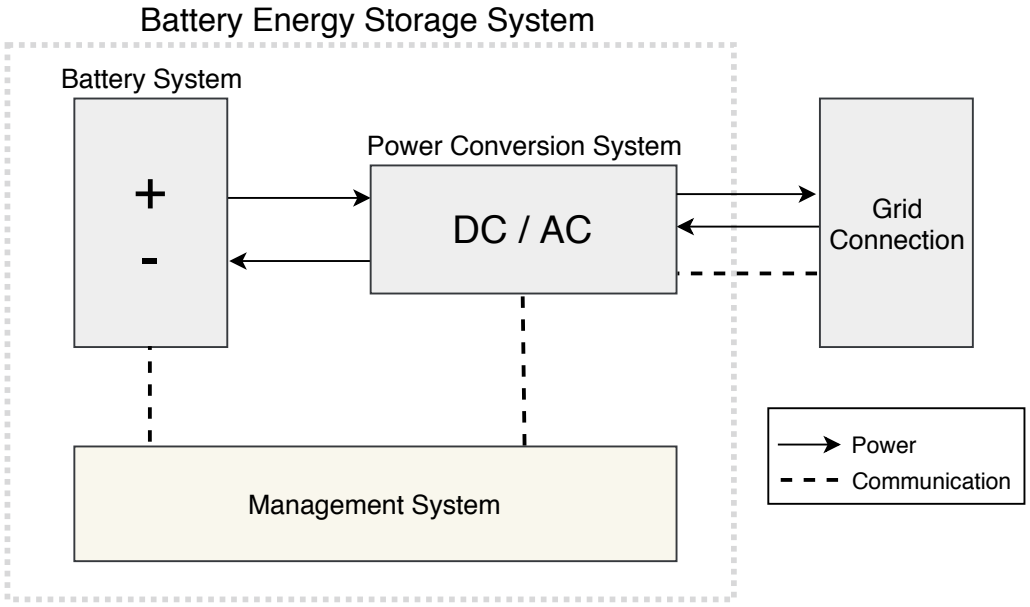

Figure 4.1: Configuration of a typical battery energy storage system with connection to the grid. It consists of a battery system, power conversion system and a management system.

4.1 BESS Projects Globally

The perceived vast potential of BESS has driven the development and deployment of such technologies and there are currently several projects around the world involving grid applications [5], [11]. The U.S. Department of Energy administers a global database listing up-to-date information regarding projects related to grid-connected storage systems. Information from [11] is used to assess current battery energy storage uses and applications around the world.

BESS projects associated with frequency regulation, in operation or under construction, with rated power over 1 MW found in [11] were studied. It is found that most projects are in the United States, Germany, Italy, and China. The most common technology types are shown in Table 4.1.

Table 4.1: Global battery energy storage projects over 1 MW by technology type. Based on information from [11].

Technology type	[%]
Lithium-ion based	78.3
Sodium-Sulfur	8.9
Lead-Acid	8.3
Vanadium-Flow	3.2
Other	1.3

As seen in Table 4.1, by far the most common technology type is lithium-based. Different types of sodium-sulfur, vanadium-flow and lead-acid technologies are also used.

One outstanding example of a battery storage project is the Hornsdale Power Reserve. It is the largest operational BESS, located in Australia connected to Hornsdale Power Reserve wind farm [11]. It is a lithium-ion battery storage system provided by Tesla with 100 MW / 129 MWh capacity. 70 MW out of its total capacity can run for 10 minutes and is dedicated to frequency regulation by maintaining system stability and security [29]. The other 30 MW can run for three hours and is designed for load shifting [29]. The battery storage system has been in operation since December 01, 2017 and has during that time proven to be capable of providing both frequency regulation and load shifting [11], [29].

More large scale projects are announced and on the way, fueled by government initiatives and incentives. As mentioned in subsection 3.2.5, a new ancillary service has been created in Great Britain to encourage development of BESS and in Korea several large-scale BESS projects are announced [7].

The trend indicated in Table 4.1, where lithium-based technology is the preferred type, seems to continue. Through analyzing the data from [11], it is also concluded that most BESS are not dedicated to simply one power system application. Common services other than frequency regulation are voltage and transmission support,

congestion relief, load and generation shifting, renewable energy integration, black start, and ramping.

4.2 Battery Systems

A battery in simple terms converts electrical energy into chemical energy when charged, and the other way around when discharged [30]. Battery systems consist of electrochemical cells with electrodes and electrolytes [10], [33]. In this section specifications describing characteristics of batteries are introduced. Battery technologies that are used or could prove useful in power system applications for frequency regulation are also presented.

4.2.1 Battery Specifications

The following is a summary of common definitions from [30] used to describe the most vital characteristics and specification of battery systems for BESS.

A battery system is a type of high voltage battery pack, which is built up of modules and cells. A battery cell is the fundamental form of a battery, and modules consist of several cells connected in series and parallel. The battery pack is then constructed using modules connected in series and parallel. There is therefore no essential difference between a small or large battery except for the amount and configuration of cells and modules [30].

State of charge (SOC) is a linear function of battery capacity given in percentage, indicating available battery capacity. SOC of 100 % indicates a battery that is fully charged, and 0 % a discharged battery. Depth of discharge (DOD) is 100 - SOC, showing how much of a battery is or will be discharged. An 80 % DOD from a battery with SOC of 90 % results in 10 % SOC. DOD is also used as a limit of maximum depth at which the battery can be discharged without severely affecting the capacity and performance.

Cycle life of a battery is a given number of charge and discharge cycles for a specific DOD and charge-discharge condition. Mainly the number of cycles and the depth of which it is discharged, affects the lifetime of a battery. Optimizing management and control of charge-discharge rate and DOD increases the lifetime of a battery [31].

Capacity of a battery is the total amount of energy, given in megawatt-hours (MWh), available when it is discharged at a certain discharge current (given as C-rate) from 100 SOC to cut-off voltage. Cut-off voltage is the voltage level at which a battery is considered empty. C-rate is the discharge current normalized to battery capacity. For a battery with 100 MWh, 1C rate means that the entire battery capacity will be discharged in 1 hour. C-rate can also be used as a limit of maximum continuous discharge current set to protect the battery from damage and reduction in capacity.

4.2.2 Lead-acid Battery Systems

Lead-acid is the most mature rechargeable battery technology available and it is considered to be reliable, cheap and has long operational life [5], [9], [32]. In power system applications it has primarily been used as an uninterruptible power supply to provide back-up power, but other applications such as frequency regulation are also recognized [5], [9], [32].

Lead-acid batteries conventionally utilize lead and lead dioxide as electrodes and electrolyte consisting of sulfuric acid [9]. The production of lead-acid batteries is well established and the recycling rate is high but with the materials used there is an elevated risk of environmental pollution [5], [9], [32]. The materials used in lead-acid batteries are toxic, hazardous, flammable and explosive, which has limited its deployment in power system applications [5], [10], [32].

Despite being cheap and widely used, conventional lead-acid batteries also have limited performance. The technology suffers from low energy and power density, long charge time and high self-discharge rate. It also suffers serious loss in capacity following deep DOD or rapid discharge [5], [33]. The main advantages and disadvantages of lead-acid batteries are shown in Table 4.2.

Table 4.2: Main advantages and disadvantages of lead-acid battery systems.

Advantages	**Disadvantages**
+ Reliable	- High risk of environmental pollution
+ Low cost	- Low efficiency
+ Mature	- High self-discharge
+ Long operation life	- Limited depth of discharge

Research in lead-acid technology has resulted in the development of advanced lead-acid batteries. Modifying the chemistry of the negative electrode by adding carbon has shown to significantly improve characteristics in terms of cycle life, charge rate, and power density [5], [9], [33]. The deployment of advanced lead-acid batteries is currently not well established [11].

4.2.3 Vanadium-flow Battery Systems

Flow batteries consist of two cells separated by a membrane with remote storage of the separate electrolytes [5], [9]. Electron pairs solved in electrolytes are pumped through cells where the electrochemical reaction takes place on stationary electrodes [5]. Since the storage of the electrolytes is remote it is possible to have very high capacity making it well suited for large energy storage applications [9].

There are several different types of flow batteries but the most developed type is the vanadium redox flow battery [5], [9], [34]. The vanadium based flow battery utilizes the four oxidized states of vanadium contained in two separate sulfuric acid electrolytes. Electrons are conducted by changing the oxidized state of the vanadium

ions [5], [9].

The technology is considered to have high energy and power capacity, long lifetime and no limit on DOD. It is also considered to have low risk of pollution, as there are no toxic materials involved. Its major drawbacks are high construction costs and the limited available supply of crucial material for electrolytes, electrodes and membranes [5], [10]. It also suffers from low energy density compared to other battery technologies and therefore its development has been restricted with only a few ongoing projects [34], [11]. The main advantages and disadvantages of vanadium-flow batteries are shown in Table 4.3.

Table 4.3: Main advantages and disadvantages of flow battery systems.

Advantages	**Disadvantages**
+ High capacity	- High cost
+ No limit to depth of discharge	- Shortage of material
+ Long lifetime	- Low energy density
+ Low risk of pollution	- Underdeveloped technology

Current development in the area is focused on the critical materials, increasing its energy density and improving range of operating temperature, which is currently roughly 0-40 °C [10].

4.2.4 Sodium-sulfur Battery Systems

Sodium-sulfur batteries are different from most conventional rechargeable batteries as they have liquid electrodes and a solid electrolyte. Molten sodium and sulfur act as the negative and positive electrodes respectively, while the electrolyte is a solid ceramic tube separating the electrodes [5], [9]. It is a high-temperature battery operating at 300-350 °C, which is needed to keep the electrodes liquefied [5], [10].

Sodium and sulfur are both inexpensive, environmentally safe and abundant materials making the batteries ideal for large scale mass production in terms of material [9]. The batteries have high energy density and high efficiency. They also have proved useful in power system application, especially for load leveling [10], [9].

The main disadvantages are related to practical issues. With an operating temperature of 300-350 °C fires are of higher risk and therefore safety is important aspect [5], [10]. The operating temperature also enhances corrosion of the compound materials. With a fragile electrolyte, it suffers from regular breakdowns caused by vibrations in certain applications, e.g. mobile applications [5], [9]. This could on the other hand, indicate it is better suited for stationary power system applications.

Insulation and temperature management is expensive and to benefit from the cheap and large supply of raw material, large units are required [9]. The cost and the safety risks has so far limited its further development [5]. The main advantages and disadvantages of sodium-sulfur batteries are shown in Table 4.4.

Table 4.4: Main advantages and disadvantages of sodium-sulfur battery systems.

Advantages	Disadvantages
+ Abundance of materials	- High operating temperature
+ Cheap	- Safety risks
+ High energy density	- Corrosion
+ High efficiency	

Research is mainly focused on lowering the operating temperature to reduce safety concerns and corrosion issues [5], [10].

4.2.5 Lithium-ion Battery Systems

As shown in Table 4.1 in section 4.1, lithium-ion based batteries are the most common grid connected battery type used today. Lithium-ion is superior over other technologies in terms of efficiency, energy and power capacity and density [9], [10], [31], [33]. This makes them well suited for their current application in mobile phones, vehicles, and in power systems [5], [10], [33].

Lithium-ion batteries usually consist of a graphite anode, a lithium metal oxide cathode based on cobalt, and an electrolyte of organic liquid with lithium salt [10], [9]. The electrodes have highly porous structures with many layers enabling extensive storage of lithium-ions [35]. This ability to host ions explains why lithium-ion batteries have the highest energy densities of all battery technologies [31].

Despite the mentioned advantages the main challenges are with the production costs, which restricts their utilization in power systems [10]. The most expensive component in a lithium-ion battery is the cathode, where cobalt is the most expensive material [31]. The complicated process of developing the electrodes and electrolyte also adds to the expenses [5]. Currently significant effort is put in to lower the production costs but there are growing concerns regarding the supply of materials, forcing developers to look at alternative materials [10].

Another drawback is the safety concern relating to overheating. When lithium-ion batteries are subject to overcharging or when internal short circuits occur the temperature increases [5], [9]. The high-energy density and flammable material creates a risk of explosion. Therefore, protection against excessive voltages, current and temperature is required to guarantee safety [10]. The main advantages and disadvantages of lithium-ion batteries are shown in Table 4.5.

Table 4.5: Main advantages and disadvantages of lithium-ion battery systems.

Advantages	Disadvantages
+ Commercialized	- High cost
+ High efficiency	- Limited supply of materials
+ High capacity	- Safety risks
	- Limited lifetime

Research is focused on increasing cycle life, lowering costs by introducing economy of scale, and finding lower cost alternatives for certain materials [5], [10], [9]. Decreasing costs and improving cycle life is vital to enable wider use of lithium-ion battery systems in power systems.

4.2.6 Aging Mechanism of Lithium-ion Batteries

To accurately model BESS dynamic frequency regulation and attempt to achieve ideal control over operation there is a need to understand aging mechanisms of batteries. Batteries degrade over time and suffer power and energy loss, a result of increased resistance and reduced capacity [31]. Aging is clearly correlated to the usage and operation of the battery system and to understand critical mechanisms it is also necessary to understand basic operation concepts [31].

When a lithium-ion battery is charged, the anode has high concentration of ions and low potential. At the same time, the cathode has low concentration of ions and high potential [36]. High SOC corresponds to high cell voltage, and low SOC to low cell voltage. When the electrodes are connected externally, to preserve charge neutrality, lithium-ions are simultaneously moved by the electrolyte from anode, through a separator, to the cathode [36]. The spontaneous movement of electrons from anode to cathode conducts current. This reduces the cell voltage and discharges the battery [5], [31]. The reversed process is that of charging [36].

Battery energy output depends on operating voltage, storage capacity of lithium-ions and internal resistance [31]. Lower storage capacity is a result of loss of lithium-ions and reduced hosting capabilities of the electrodes. This is caused by side reactions with lithium-ions, changes in electrode structure, and loss of active electrode material [31]. Increased internal resistance reduces the battery's ability to transport lithium-ions and results in slower discharge and charge processes [36]. Internal resistance is made up of impedance contributions from many different sources: contact resistance, charge transfer, diffusion, ohmic losses and electrical resistance of the electrolyte [31]. The major cause of aging in lithium-ion batteries is increased charge transfer resistance between electrodes and the electrolyte [31].

Lithium-ion cells also experience aging when they are not in operation, which is called calendar aging [31]. The main contribution to calendar aging is increased contact resistance between the graphite anode and electrolyte, which is caused by growth in a passive surface layer, called solid electrolyte interphase [31], [37]. Calendar aging is heavily dependent on, and accelerated by, high surrounding temperature and SOC.

4.3 Power Conversion Systems

A power conversion system (PCS) is the connection of the battery system to the grid, managing conversion of both AC-DC and DC-AC. There are two common types of PCS used in BESS applications.

The first PCS is a simple single-stage bi-directional AC-DC converter [5], [38]. One of many different designs and topologies of such a PCS is a 3-phase, 6-pulse bridge inverter. Its IGBT switches are controlled by PWM signals from the battery management system to control the power flow [38]. A single-stage AC-DC converter is usually applied to an independent power source in a distributed power generation system since it has a simple structure with high efficiency [5]. But it suffers from insufficient control over charging and discharging resulting in instability and inaccuracy [5], [38].

Another PCS topology commonly used is a two-stage AC-DC and DC-DC converter. It has better control over charging and discharging of the battery making the system more reliable and accurate [5]. The DC-DC conversion allows for efficient current limitation and the high efficiency reduces energy loss [39]. This makes it well suited for large-scale applications where current limiting and power control is important.

Research in PCS is focused on reducing switching losses, increasing efficiency and adapting it to handle higher operating temperatures to improve the overall performance [5]. However, customized solutions for BESS applications are not prioritized since available power electronic converter technology can easily be adapted to be used in BESS [5], [38].

4.4 Battery Management Systems

The battery management system (BMS) is needed to monitor and maintaining safe and ideal operation of a BESS [28], [38]. To achieve desired lifetime, improve efficiency, fulfill application requirements and because of restrictions in inherent characteristics of the battery system, cell voltage and charge/discharge current should be constantly managed by the BMS [40], [41]. Since battery systems are of modular designs, composed of cells in series and parallel, maintaining status of each cell is needed to ensure the stability and power supply of the whole battery system [5], [41].

By monitoring voltage levels the BMS protects the battery system from over-charging and reaching complete discharge [5]. Over-charging occurs when the battery system reaches too high SOC and complete discharge by too low SOC and too deep DOD. As explained in subsection 4.2.6, SOC is directly correlated to cell voltage level and both over-charging and complete discharging seriously affects battery capacity and performance [31]. The BMS also provides protection by controlling charge and discharge current, and by monitoring temperature and short circuit currents [5].

Another vital function of the BMS is to handle effective management and dispatching of power to the grid. Depending on operation setting and grid activity the BMS must manage the BESS to respond accordingly [5]. It should also fulfill connection requirements and achieve continuous communication and power exchange with the grid [42].

Gradual increase in demand for BESS and the high demand for battery systems in mobile applications has driven development and research in optimized BMS and its importance has been recognized and greatly promoted [5].

5
Swedish Transmission Grid Model

The Swedish power system model used in this thesis is a detailed transmission grid made in PSS/E capable of emulating static characteristics of the Swedish power system and dynamic frequency characteristics of the Nordic synchronous power system. It is based on a model that is the result of the master's thesis project [43]. This chapter describes the structure and behavior of the model.

5.1 Static Modeling

The model developed in master's thesis project [43] is an emulation of the Swedish transmission system, including production sources, loads, and connection points to distribution grids and external grids. It is an aggregated model with 221 buses, 478 generators, 283 branches and 193 loads. The model is limited to the grid owned by the Swedish TSO in voltages 220 kV and 400 kV for year 2015. It is divided into 20 Swedish counties, markets areas SE1-SE4 and includes connection points to Norway, Finland and Denmark.

The model is developed in PSS/E, which is a power system simulation software for engineers used for planning and analyzing transmission networks. Information was gathered solely from open source material: databases, official reports, master's thesis projects, and literature. This section summarizes the work on the static modeling presented in [43] and contributions made by the author.

5.1.1 Modeling of Generation

Installed generation capacity in the model resembles actual installed capacity in Sweden for year 2015. Comparison of the modeled capacity to actual capacity is shown in Table 5.1, based on official data from the Swedish Energy Agency [44].

Table 5.1: Installed capacity in Sweden for 2015 compared to modeled capacity by types of production sources.

Type	**Installed capacity [MW]**	**Modeled capacity [MW]**
Hydro	16 184	16 312
Nuclear	9 714	9 076
Thermal	7 920	7 920
Wind	6 029	1 940
Solar	104	0
Total	39 951	35 248

The difference in actual installed capacity and modeled installed capacity is in detail explained in [43]. The most significant difference is in wind power. This is the result of only including the largest wind farms in Sweden and excluding individual wind turbine units, as this was deemed too time consuming [43].

5.1.2 Modeling of Loads

System loads are modeled as directly connected to the buses to represent connections to distribution grids and consumption. Loads are modeled as pure active power loads based on the statement that the Swedish TSO aims to have zero sum exchange of reactive power exchange during normal operation, stated in [45].

When simulating static load flow, the hourly consumption for each market area, obtained from Nord Pool database [46], is distributed among buses in the model based on annual county consumption. This is an approximate approach requiring adjustments to achieve correct balance in the system. To reach the desired consumption in each market area loads were moved from one market area to another by scaling loads during the validation process, later explained in section 5.2.

5.1.3 Modeling of Transmission Lines

Transmission lines and the connection points to substations in the grid are based on the European grid map from ENTSO-E [47]. As described in [43], this information allowed modeling of transmission lines and substations with high similarity to the actual Swedish transmission grid. All lines are assumed to be overhead lines of the same material and type, based on information from [48]. The resulting PSS/E graphical layout is shown in Figure 5.1.

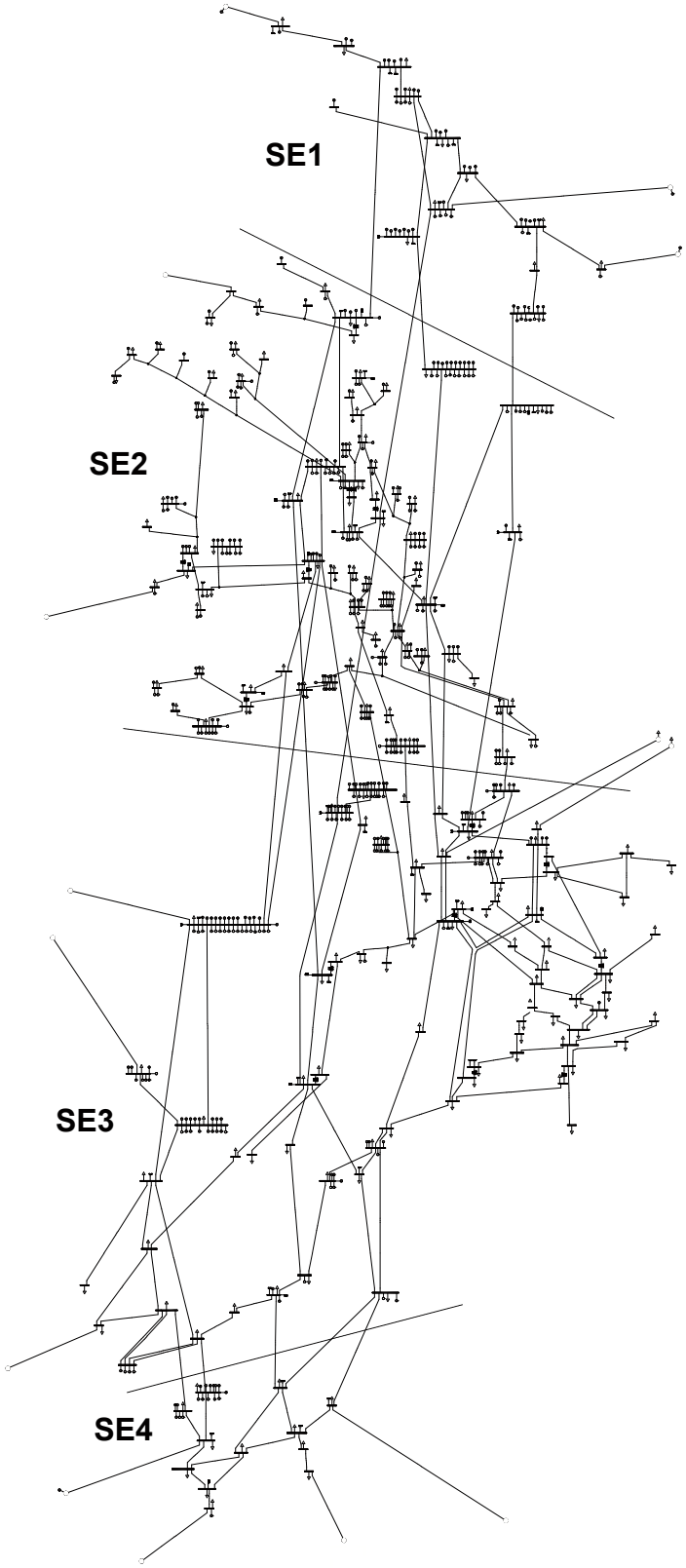

Figure 5.1: The graphical layout of the Swedish Transmission grid modeled in PSS/E and first presented in [43]. The four market areas SE1-SE4 are separated by solid lines. The Ringhals bus is in the south west part of SE3 and the swing bus is located in the middle of SE2.

5.1.4 External Connections

There are 14 connections to external grids included in the model, in the form of transmission lines of 220 kV and 400 kV, and HVDC links. AC external connections are modeled with generating units and HVDC lines and associated connections are modeled as active power loads. Generating units and loads supply and consume power to indicate import and export to and from Sweden.

5.2 Validation of Static Model

The static model was validated using recorded load flow data from Nord Pool. One high and one low demand case was examined in [43], and an additional high load case is introduced in this thesis. Data for each case includes: production, consumption and power flow in and between market areas SE1-SE4, import and export to and from Sweden, and production by power source type.

The case introduced in this thesis is hour 10:00-11:00 on March 05, 2015. This case was chosen as it provides a reference frequency response, which is crucial for verifying the dynamic characteristics of the model. The case has 21 566 MW recorded production, 20 446 MW demand (including losses) and net export of 1 011 MW. Result of load flow simulation is shown in Table 5.2.

Table 5.2: Actual and modeled production, demand, and exchange for the market areas, and export to different countries, on March 05, 10:00-11:00, using recorded historical data from Nord Pool [46].

	Area	**Historical [MW]**	**Modeled [MW]**
Production	SE1	3 821	3 821
	SE2	6 667	6 559
	SE3	10 313	10 313
	SE4	764	764
	Total	21 566	21 457
Demand	SE1	1 288	1 288
	SE2	2 418	2 418
	SE3	12 912	12 912
	SE4	3 828	3 828
	Total	20 446	20 446
Export	NO	-2 563	-2 563
	FI	2 587	2 587
	DK	58	58
	PL	603	603
	DE	326	326
	Total	1 011	1 011
Exchange	SE2-SE1	1 295	1 308
	SE3-SE2	5 727	5 646
	SE4-SE3	4 296	4 316

As seen in Table 5.2, correlation between actual recorded and modeled production, consumption, export and exchange is high. The difference between modeled production and historical production is caused by the imbalance from the source data, which results in reduced production in SE2. Both demand and export are modeled with complete correlation to the recorded historical data. Deviation in exchange between market areas is most likely caused by imprecise division of loads and production units not entirely correlating to the market areas.

Validation using recorded historical data from Nord Pool demonstrates that the model used in this thesis can emulate the load flow of the Swedish transmission grid, with only a small degree of deviation.

5.3 Dynamic Modeling

The aim of dynamic modeling is, in this thesis, to correlate the frequency response of the model following a major disturbance to the real response of the Nordic power system. As the dynamic simulation of frequency response was at first insufficient, several contributions to the model were made.

As noted in [43], the process of developing a dynamic model of the Swedish power system is demanding and acquiring necessary data is difficult. The dynamic characteristics were obtained through contacts with experienced people in the industry, from thesis [49] and model Nordic44. The raw and processed data files corresponding to model Nordic44 are available as an open data set documented in [50] and it is first presented in [51].

5.3.1 Generation Units

To simplify and facilitate dynamic modeling, production units of the same type are assigned the same models and associated variables. The PSS/E dynamic models used for generator, exciter and stabilizer characteristics are presented in Table 5.3.

Table 5.3: Generating units their assigned dynamic models in PSS/E.

Unit Type	Generator	Exciter	Stabilizer
Hydro	GENSAL	SCRX	STAB1
Nuclear	GENROU	SCRX	STAB1
Thermal	GENROU	IEEET2	STAB1
External Connection	GENSAL	SCRX	STAB1

GENSAL is a salient pole generator model used for hydro units. GENROU is a round rotor generator model for both nuclear and other thermal generators. The units representing external connections to Norway, Finland and Denmark in Table 5.3 are assigned the same models as hydro units, GENSAL. This is to enable and facilitate modeling of external frequency contribution.

Wind power units are not included in Table 5.3. All wind turbines are assumed to be variable speed wind turbines, and should not contribute with system inertia [23]. This was implemented using the PSS/E function GNET. Activity GNET replaces generation units with equivalent negative load [53]. With wind turbines modeled as negative loads they will not contribute with inertia, as expected from variable speed wind turbines. This is a relatively basic solution but for the purpose and aim of this thesis it is deemed sufficient. An alternative solution would be to find appropriate dynamic wind turbine models and parameters, which could be useful for further studies related to dynamic characteristics and synthetic inertia from wind turbines.

5.3.2 Load Conversion Factors

When performing dynamic simulations of the Nordic power system in PSS/E loads are in most cases converted to either constant current, constant admittance or constant power loads, or a mix of all three [49], [54]. The load conversion factor is used model the dynamic behavior of loads. Different TSOs use different load conversion factors and load conversion factors used by current the Swedish TSO Svenska Kraftnät to perform dynamic simulations in PSS/E, are 0/40/60 for active power and 0/90/10 for reactive power [54]. The same conversion factors are consequently used in this thesis.

5.3.3 Inertia Constants and System Inertia

Modeling of system inertia is important for the model to possess the desired characteristics of the Nordic power system. Inertia constants and system kinetic energy assigned in [43] to the model was therefore carefully reexamined and additional approximations were made.

Given active power capacity the machine bases S_g in (MVA) were calculated assuming generators operating at power factor 0.9. The principle values, from [55] shown in Table 5.4, are used to assign inertia constants to generators in the model.

Table 5.4: Proposed inertia constants (H_g) for different generator types from [55].

Generation type	H_g [s]
Nuclear	6.4
Hydro	3.4
Thermal	2.8
Wind	0.0

With the calculated generator bases S_g and the inertia constants H_g shown in Table 5.4, system kinetic energy capacity can be calculated. Using equation (3.4), the kinetic energy capacity in Sweden is estimated to 154 900 MWs.

In [12] the kinetic energy capacity of Sweden is estimated to roughly 156 400 MWs. Comparing the calculated value 154 900 MWs and the estimated kinetic energy in

Sweden 156 400 MWs, indicates that the principle inertia constants used and assumptions made are reasonable.

The kinetic energy capacity and distribution per country, from the estimations in [12], are shown in Table 5.5.

Table 5.5: Kinetic energy capacity in Sweden, Norway, Finland and Denmark and distribution, based on estimations from [12].

Country	**Kinetic energy [MWs]**	**Distribution** [%]
Sweden	156 400	45.0
Norway	97 500	28.1
Finland	74 200	21.4
Denmark	19 300	5.6
Total	347 500	100

The kinetic energy in the Nordic power system for the case on 05 March 2015 used in section 5.2 is estimated to roughly 260 000 MWs using [12] and [1]. With the distribution presented in Table 5.5, inertia in each country can be estimated.

Kinetic energy in the Swedish model is calculated to roughly 119 800 MWs from the load flow simulation conducted in section 5.2. To reach desired level of kinetic energy in the Nordic system, remaining kinetic energy is distributed to each country according to the distribution shown in Table 5.5. This is done by adjusting M_{base} and inertia constant H_g for generating units representing connection points to external grids.

The resulting approximated and modeled kinetic energy E_k distribution in the Nordic power system is shown in Table 5.6.

Table 5.6: Estimated and modeled kinetic energy E_k in Sweden, Norway, Finland and Denmark for March 05, 10:00-11:00, based on estimations from [12], [1].

Country	**Estimated** E_k **[MWs]**	**Modeled** E_k **[MWs]**
Sweden	117 000	119 800
Norway	73 100	71 500
Finland	55 600	54 500
Denmark	14 600	14 200
Total	260 000	260 000

To simulate a realistic load flow scenario with production of each unit over 80 % and to achieve desired level of kinetic energy not all generators in the model are in service. As it is an aggregated model, completely balancing estimated and modeled kinetic energy was not possible and the difference in kinetic energy is deemed acceptable.

5.3.4 Turbine Governors

Dynamic simulation of generating units was completed by implementing PSS/E models of turbine governors. The focus was on turbine governors for hydro units as these are the major source of frequency reserve in the Nordic Power system [49]. Nuclear power is not used for FCR-N or FCR-D and there is limited amount of thermal power production active in the case chosen. Therefore, in the model only hydro units are active in primary regulation.

The governor model IEESGO is used for nuclear and other thermal units, as suggested in [49], [50]. It is a general-purpose turbine able to provide a good representation of a reheat steam turbine [56]. The frequency regulation capability of this model was inactivated and as desired the units do not act in primary frequency regulation and do not provide FCR.

The turbine model WEHGOV is used to model hydro units as it is a detailed turbine model with a PI regulator. Modern governors today are electronic and it is argued that a PI controlled governor model is to prefer when modeling modern hydro unit frequency characteristics [49], [57]. WEHGOV is a representation of a Woodward Electronic hydro-governor [56]. The parameters for the variables of WEHGOV used in the model in PSS/E, were acquired from contacts in the industry, a study presented in [58], and by using typical values presented in [56].

5.4 Validation of Dynamic Model

The case 10:00-11:00 on 05 March 2015 was chosen as it provides a reference frequency response of the Nordic power system. On March 5, at approximately 11.04 Ringhals 4 was disconnected. This resulted in a frequency deviation and frequency response as shown in Figure 5.2, as presented in [49].

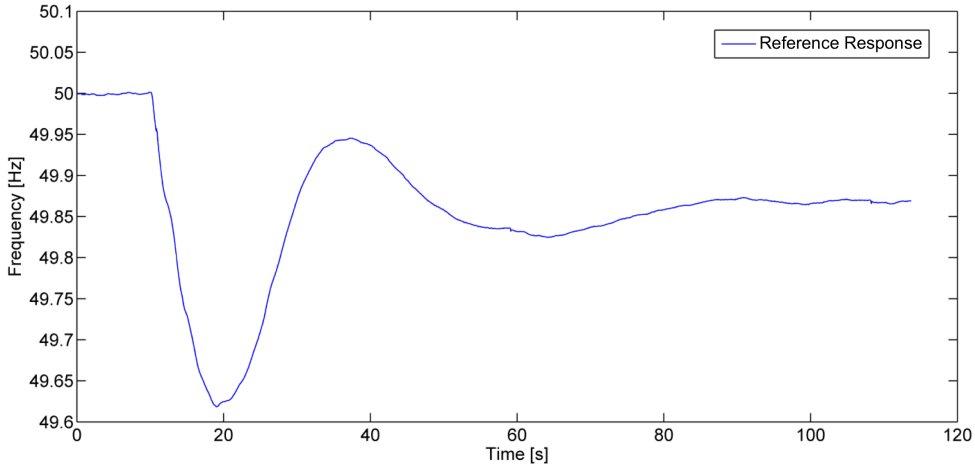

Figure 5.2: Reference response of Nordic power system on 05 March 2015, as presented in [49]. At 10 seconds, Ringhals 4 was disconnected resulting in a large frequency deviation from 50 Hz down to 49.62 Hz with steady state frequency at 49.87 Hz.

As seen in Figure 5.2, the outage of 1110 MW occurring at 10 seconds, results in a large frequency deviation. Frequency drops as low as 49.618 Hz at 18.92 seconds and is stabilized at roughly $f_{ss} = 49.87$ Hz. This response and provided values from [49] are used to achieve the desired frequency regulation and to verify the dynamic model behavior. Given the steady state frequency f_{ss} and the power deficiency, the system frequency response is calculated using equation (3.9), resulting in total frequency response of approximately 8540 MW/Hz.

The total frequency response of 8540 MW/Hz was distributed to Sweden, Norway, Finland and Denmark based on the FCR-D requirements set by the Nordic System Operation Agreement, previously mentioned in subsection 3.2.2 and the distribution used in [49]. The resulting contribution from each country in the model is shown in Table 5.7.

Table 5.7: Frequency response contribution from Sweden, Norway, Finland and Denmark in the model for the frequency event on March 05, 2015. Distributed using the reference case in [49] and according to FCR-D requirements set by the Nordic System Operation Agreement.

Country	**Frequency response [MW/Hz]**
Sweden	2 860
Norway	2 980
Finland	1 800
Denmark	700
Total	8540

The frequency contribution from each country is like the distribution given in SOA but adjusted to better represent a realistic distribution. This is achieved by increasing contribution from Norway in accordance with the reference case.

After distributing the frequency response contribution, parameters of turbine governor WEHGOV were adjusted by altering proportional and integral gain parameters K_P and K_I to achieve desired frequency regulation. The resulting modeled frequency regulation and reference frequency regulation are shown in Figure 5.3.

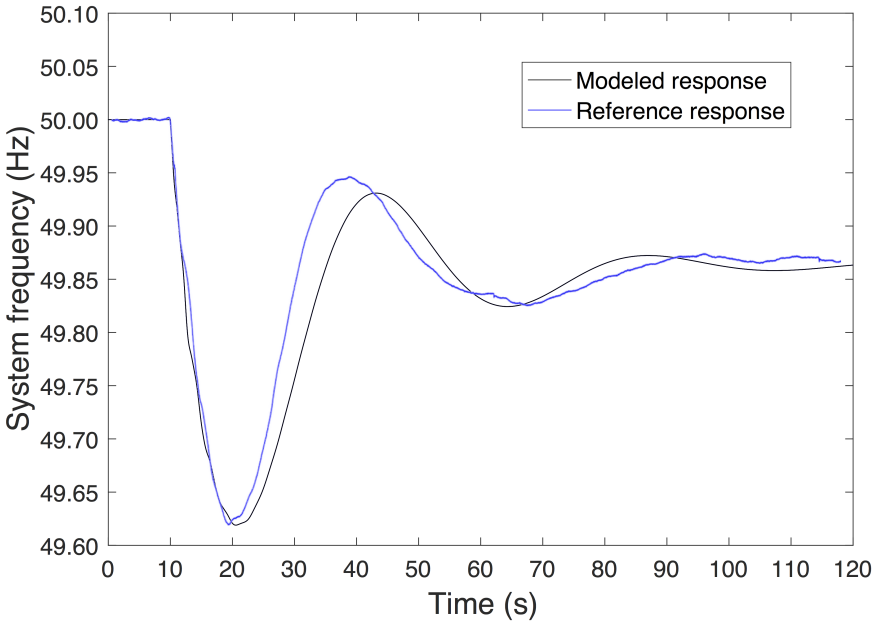

Figure 5.3: Frequency regulation of model and reference case following a production loss of 1110 MW on March 05, 2015.

Modeled frequency regulation is similar to the reference case, as seen in Figure 5.3. Both reference and modeled frequency deviation reach the same minimum frequency of about 49.62 Hz and steady state frequency of 49.87 Hz. The model does not recover as quickly as the reference and oscillates longer. The oscillations are most likely caused by having very strong frequency response and many generators reacting to the frequency deviation. This could be adjusted by setting some turbine governors as offline but would also require reassigning the frequency response contribution in order to achieve desired steady state frequency, a time-consuming process.

With the assumptions made and considering an aggregated model is used, deviations from the reference case are expected. The resulting frequency behavior of the model, illustrated in 5.3, is regarded as adequate for this thesis.

5.5 Reduced Kinetic Energy and Model Behavior

To illustrate the importance of system inertia and kinetic energy and the effect it has on the Nordic power system frequency, reduced inertia simulations were conducted using the dynamic model. These simulations were also used to verify that the model behaves as it should by comparing results to similar studies on reduced inertia in

the Nordic power system, in [1], [2], [49].

A low load case, e.g. a summer night with high wind production and import through HVDC links, is when reduced inertia is expected to have the largest impact on the power system [1], [2], [23]. But as explained in section 5.2, a reference frequency response was needed to validate the model and no such reference case for a summer night was found in open sources. Instead the same load case of 10:00-11:00 on March 05, 2015 and production loss of 1110 MW, as in section 5.4, was chosen for these simulations. In future work, it would be interesting to look at a low load reference frequency response case to see how reduced inertia effects the Nordic power system.

Simulations were conducted by reducing modeled kinetic energy from initial 260 000 MWs to 130 000 MWs, and down to 80 000 MWs, to see the effects on system frequency deviation. 260 000 MWs corresponds to roughly system inertia constant 5 s. 130 000 MWs is roughly the lowest level of kinetic energy in the Nordic power system today corresponding to an inertia constant of roughly 2.5 s. [1]. This also corresponds to the kinetic energy from approximately twice the installed nuclear capacity in Sweden. 80 000 MWs was chosen as it was estimated in [12] to be the lowest level of kinetic energy in the future Nordic power system and corresponds to a system inertia constant of 1.5 s. The resulting behavior is shown in Figure 5.4.

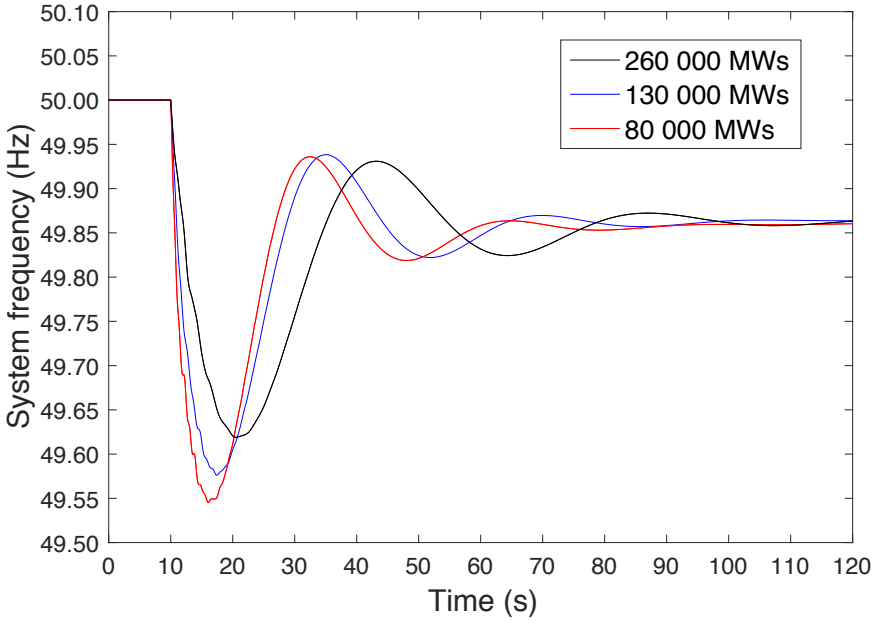

Figure 5.4: Illustrating change in frequency deviation by reducing kinetic energy in the modeled system from 260 000 MWs, to 130 000 MWs and 80 000 MWs.

As seen in Figure 5.4 reducing inertia results in steeper frequency decline, lower frequency nadir and reduced time to frequency nadir. The lowest point of frequency is referred to as frequency nadir in [23], [49], [59]. The results shown in Figure 5.4 corresponds to the results of studies [1] and [2].

For the model used in [1], illustrated in Figure 5.9 in [1], reducing system kinetic energy from 130 000 MWs to 86 000 MWs results in a 1.2 Hz reduction in frequency nadir and roughly 2 second difference in time to nadir. In Figure 5.4, time to nadir is reduced roughly 2 seconds when kinetic energy is reduced from 130 000 to 80 000 MWs but difference in frequency nadir is only 0.6 Hz. However, considering the considerable amount of frequency regulation at 8540 MW/Hz and having many generators regulating system frequency, these results are regarded as reasonable.

Theoretical values of rate of change of frequency (RoCoF) measured in Hz/s for the different simulated cases were calculated using equation (3.7) and are shown in Table 5.8.

Table 5.8: Theoretical values of rate of change of frequency for the simulated cases.

System inertia [MWs]	RoCoF [Hz/s]
260 000	0.11
130 000	0.21
80 000	0.35

To better illustrate how reducing inertia results in steeper frequency decline and how it affects RoCoF, the first second of after the production loss is examined. This is shown in Figure 5.5.

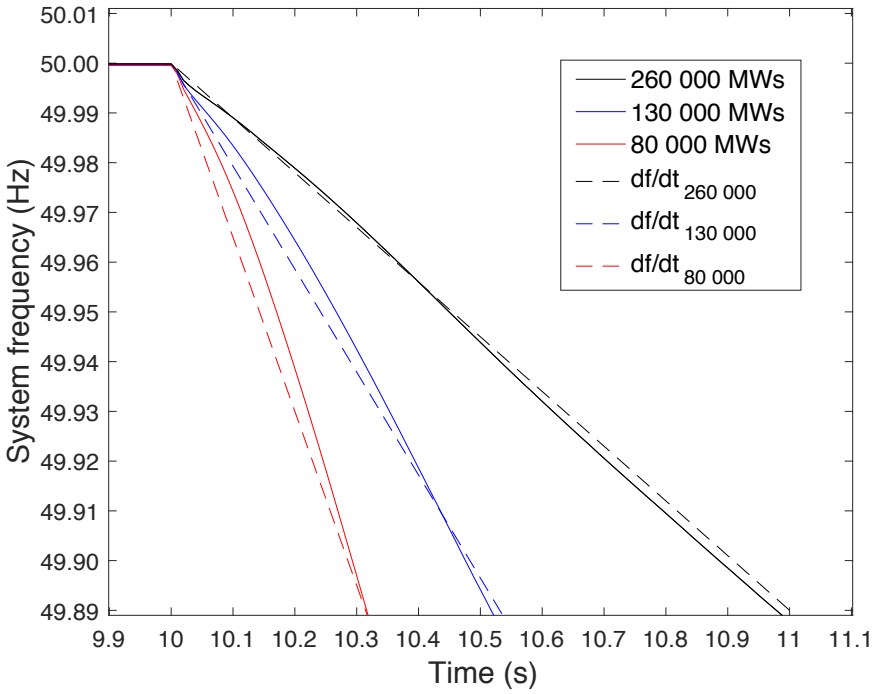

Figure 5.5: Illustrating the effects of reduced kinetic energy on rate of change of frequency for a major fault. Reducing inertia results in increased frequency decline. The solid lines show the frequency of the model and the dashed lines show the theoretical frequency decline.

Figure 5.5, shows the theoretical and modeled frequency decline following the loss of production. The theoretical values of RoCoF for the different kinetic energy cases are represented in Figure 5.5 by the dashed lines $\mathrm{dfdt}_{260\,000}$, $\mathrm{dfdt}_{130\,000}$ and $\mathrm{dfdt}_{80\,000}$. In this example the load frequency dependence and turbine governors have been removed to show the unregulated RoCoF and to illustrate the correlation of the model to theoretical RoCoF without damping.

Right after the fault is introduced at 10 seconds, the same frequency decline is shown for all three kinetic energy cases until roughly time 10.02 s. Also, the frequency decline is not linear. In [60], it is suggested that PSS/E calculates dynamic frequency based on bus voltage angle using a low-pass filter, which results in distortion. This might also be caused by rotor angle instability caused by the disturbance. In [60], roughly 0.3 seconds is required before the frequency output is as expected and in this thesis slightly longer time seems to be needed. This non-linearity is also observed in other studies of frequency decline using PSS/E, such as [54]. Despite the initial non-linearity, the response of the model correlates well with theory and other reference results.

6
Modeling Battery Storage Systems

This chapter describes the process of modeling components and dynamic characteristics of BESS in PSS/E. The outcome is two different user-defined dynamic models, which are not part of the PSS/E library of provided dynamic models.

6.1 Choosing Suitable Technology

Choosing a battery system suitable for the intended application in the Nordic power system is accomplished by matching specified requirements with key parameters of the different battery technologies. For frequency regulation applications, long cycle life is critical as discharge events occur repeatedly, and long service life is crucial for long-term pay-off. High energy conversion efficiency, discharge current and rapid response of the BESS are required to enable delivery of full power to the grid in a short period of time [5].

Information from [5], [9], [10] was used to summarize key parameters of the battery technologies introduced in section 4.2. Main parameters considered are cycle life, energy efficiency, cost, and maturity. Cycle life is the number of charge-discharge cycles the battery handles before capacity is reduced below 80 % [31]. Efficiency is the round-trip efficiency of the battery and cost is per kWh. These parameters shown in Table 6.1 for each battery technology.

Table 6.1: Key parameters of different battery energy storage technologies [5], [9], [10].

Type	Cycles	Efficiency	Cost (SEK/kWh)	Maturity
Lead-acid	200 - 2000	75-90 %	1700 - 5000	Mature
Vanadium-flow	10 000 - 18 000	70-85 %	5000 - 12 500	Developing
Sodium-sulfur	1500 - 5000	75-92 %	5000 - 25 000	Commercializing
Lithium-ion	1000 - 10 000	90-95 %	10 000 - 33 500	Commercialized

Energy and power density are not limiting for stationary applications and are not included in Table 6.1. Environmental and sustainable aspects for the different technologies are not included in Table 6.1 but they are equally important as the key parameters to consider when choosing a suitable technology.

By comparing key parameters shown in Table 6.1 and environmental aspects to

the requirements for frequency regulation applications, the most suitable technology is considered to be lithium-ion. It has superior efficiency and long cycle life, both of which are crucial for the intended application. It does however suffer from some fire safety issues. The other proposed technologies suffer from major disadvantages. Lead-acid has high risk of serious environmental pollution and vanadium-flow is currently underdeveloped and has lower response time than lithium-ion systems [9].

Sodium-sulfur might be viable option in the future if shortage of material is a limiting factor for further development of lithium-ion batteries. It is significantly cheaper and has relatively high efficiency, but currently suffers from practical obstacles in terms of its high operation temperature. It is also associated with significant safety issues and the technology is not yet commercialized.

Adding to the benefits of lithium-ion technology is that safety issues are manageable and power output can be accurately controlled. Another major advantage is that the technology is already commercialized, which is crucial for its deployment in this application. However, the major drawback is concerned with high costs [10]. Expectations are that ongoing research and development in lithium-ion battery technology can bring down the costs by finding cheaper alternative materials and improving production.

6.2 Designing User Defined Models

CBEST is a dynamic model developed by Electric Power Research Institute (EPRI), and it is provided in the PSS/E model library. This dynamic battery model was at first considered to be used to model dynamic characteristics of BESS but despite being an approved dynamic model provided in the PSS/E model library, it has several limitations. Considering the limitations of the model CBEST, it was decided to develop user defined generator models of BESS.

It has been proven in studies [61], [62], [63], [64] that user defined dynamic models of BESS can be successfully created for PSS/E. The instructions provided in chapter 23 Model Writing, in [65] and discussions with experienced people in the industry were used as a guide to create the models.

Two different kinds of frequency controllers were designed, a droop control and a derivative control. The droop control is made to work as primary frequency regulation and regulates active power output of the battery in relation to frequency deviation. Derivative control functions as inertial response where it reacts to the frequency derivative and increases active power output or input in relation to the magnitude of RoCoF.

6.2.1 Droop Controlled Model

Droop control is implemented to fulfill the requirements on FCR-D in the Nordic power system. Described in subsection 3.2.2, the current principal requirements on FCR-D is that it should restrict frequency deviations from 50 ± 0.1 Hz to between 49.5 Hz and 50.5 Hz.

For a BESS to only provide FCR-D, a dead band is introduced. Within the dead band of 50 ± 0.1 Hz, battery output is 0 MW. For larger frequency deviations battery output or input is increased from 0 at 50 ± 0.1 Hz, to reach 100 % power output and input at 49.5 Hz and 50.5 Hz respectively.

To fulfill the requirements of increasing power output 100 % with a 0.4 Hz change in frequency the droop setting is set using equation (3.8). The resulting droop setting R is -0.8 (%) and the resulting proportional gain K is -125. The resulting change in BESS power to frequency with dead band is shown in Figure 6.1.

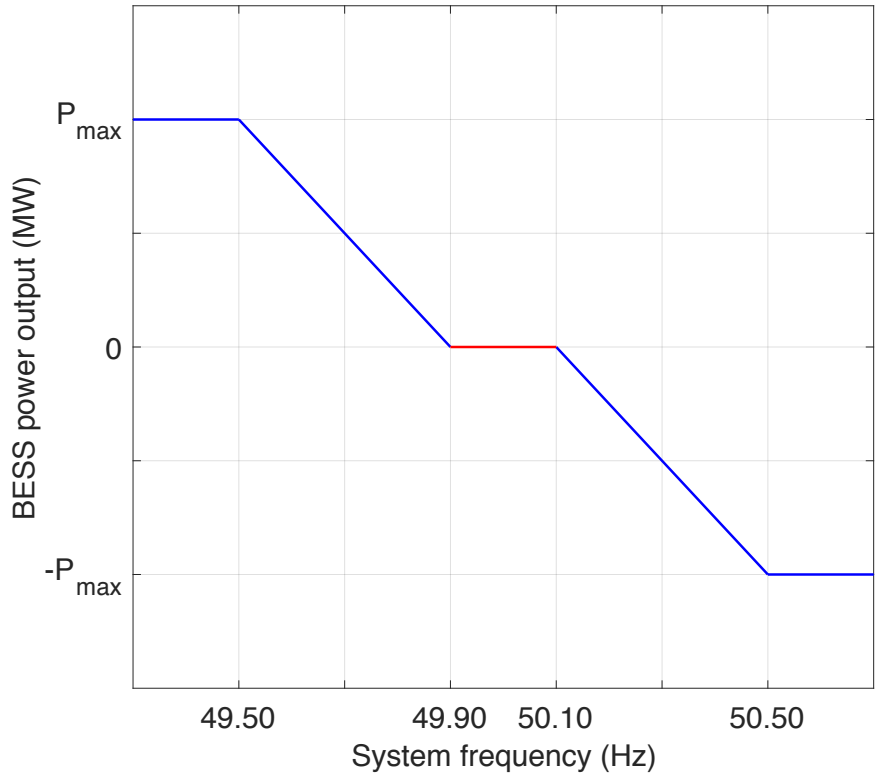

Figure 6.1: Droop setting of BESS to fulfill FCR-D requirements. Output is 0 MW for frequencies within 50 ± 0.1 Hz, shown in red. For frequencies beyond 50 ± 0.1 Hz output is increased/decreased to $\pm P_{max}$ at 50 ± 0.5 Hz, shown in blue.

In Figure 6.1 the dead band with 0 MW power output is indicated by red. Discharging or charging of the battery is increased linearly until it reaches the power limits. Maximum discharge is indicated by power output P_{max}, and maximum charging is at power output $-P_{max}$. The block diagram of the resulting droop control is shown

in Figure 6.2.

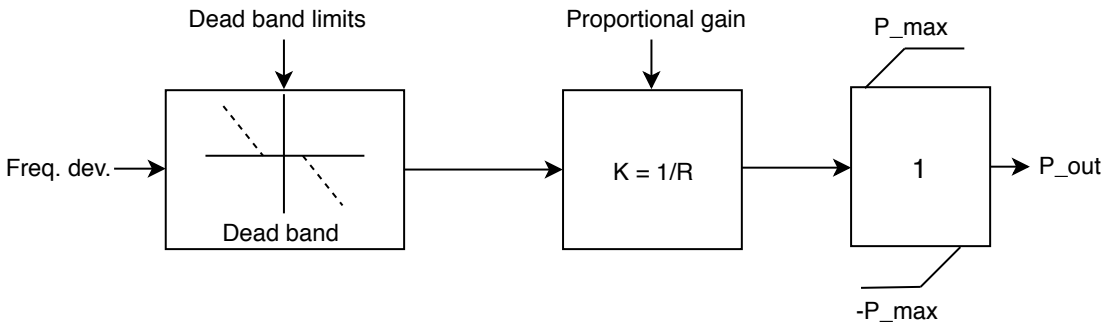

Figure 6.2: Block diagram illustrating the droop control. The frequency deviation signal Freq. dev. from the bus is passed through dead band filter with positive and negative lower limits. Then it is passed through the droop logic with gain $K = 1/R$, and then compared to maximum/minimum power output $\pm P_{max}$ to determine the resulting output signal P_{out}.

Figure 6.2 illustrates how the desired droop control is implemented in the model using the bus frequency deviation signal resulting in the power output signal P_{out}.

6.2.2 Derivative Controlled Model

In [63] it is demonstrated that a BESS with RoCoF-control can improve frequency stability in power systems as it is almost consistent with providing inertial response. As explained in subsection 3.2.1, there are currently no defined requirements on minimum inertia in the power system and there are no regulations on how it should be provided. However, there are in [4], [12], and [63], suggestions and examples on how such a controller can be implemented. The resulting derivative control model designed in this thesis is shown in Figure 6.3.

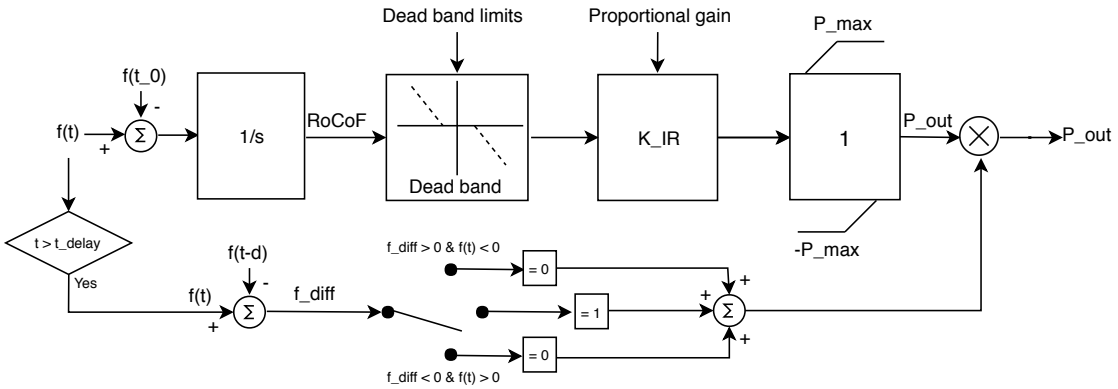

Figure 6.3: Block diagram of the derivative control model. The derivative of the difference between bus frequency $f(t)$ and frequency at the start of the frequency event $f(t_0)$, is used to calculate RoCoF. RoCoF is passed through a dead band filter, proportional gain K_{IR} is added and the output signal is then compared to maximum/minimum power limits $\pm P_{max}$ resulting in the output signal P_{out}. The lower part of the control is used when time t is larger than the time delay t_{delay}. The change in frequency at each time step f_{diff} is the difference between bus frequency $f(t)$ and the bus frequency at the previous time step $f(t-\delta)$. f_{diff} is used to determine when point of minimum or maximum frequency is reached and if it is reached power output signal is reduced to 0.

The control model introduced in this thesis, illustrated in Figure 6.3, is based on observing RoCoF, which is frequency compared to the frequency at the start of the disturbance, over time. In Figure 6.3 the BESS power output P_{out} is determined as shown in Figure 6.4.

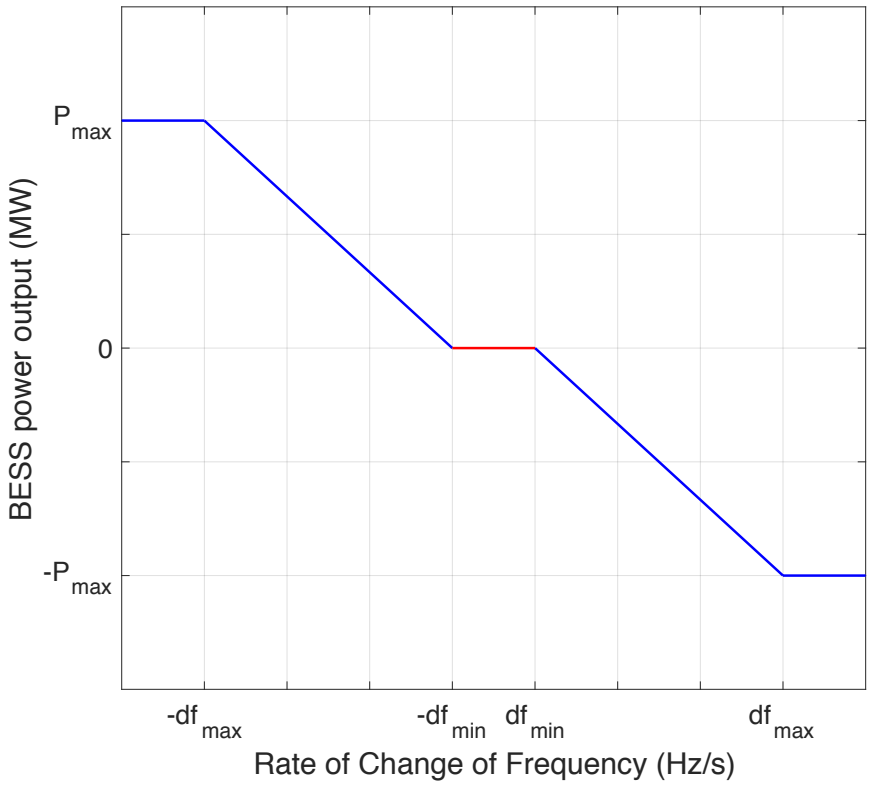

Figure 6.4: BESS power output in relation to RoCoF. Output is 0 MW for frequency derivatives smaller than ± df$_{min}$, shown in red. For frequency derivatives beyond this limit, output is increased or decreased linearly to $\pm P_{max}$ at ± df$_{max}$.

A dead band is used to ensure the BESS does not react to small frequency deviations. The lower dead band limits are indicated in Figure 6.4 as ± df$_{min}$. If they are set too low the model will react to very small deviations and if they are set too high the model might not react at all. In [63] it is suggested to set the thresholds of RoCoF control in relation to rated power of the battery used, which in that case corresponded to ± 0.072 Hz/s.

In this thesis, empirical analysis using the modeled grid was conducted to set these limits. Like the procedure in [63], different thresholds were used for different total battery power capacity. The thresholds used were ± 0.036 Hz/s for 40 MW, ± 0.034 Hz/s for 100 MW, and ± 0.027 Hz/s for 540 MW installed capacity in the grid.

Proportional gain K_{IR} is used to increase power output in proportion to RoCoF. In [4] and [63] different proportional gains are suggested. In [4] battery output is maximum at -0.5 Hz/s and in [63] at -0.3 Hz/s. It was found through tests using the modeled grid, setting of proportional gain (K_{IR}) to -10 resulted in desired response, similar to what is shown in Figure 3.2. This corresponds to maximum output at -0.10 Hz/s from the lower dead band limit, which is lower than the suggested limits of -0.5 and -0.3 Hz/s from [4] and [63]. Beyond this limit power output is restricted to $\pm P_{max}$.

Inertial response is 0 MW when system frequency reaches its maximum instantaneous frequency deviation. In the model this is implemented as shown in the lower part of the control model in Figure 6.3. But there were some difficulties because of short-term frequency oscillations at the bus where Ringhals 4 is connected. These short-term oscillations are shown in Figure 6.5.

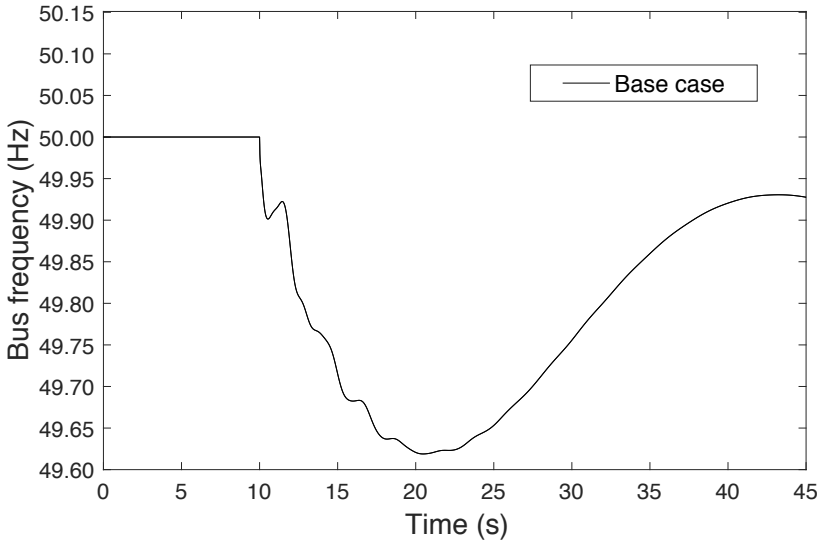

Figure 6.5: short-term frequency oscillations observed between 10 and 25 seconds at faulted bus after the trip of Ringhals 4, which occurs at 10 seconds.

Figure 6.5, illustrates how frequency oscillates for roughly 15 seconds after the production loss at Ringhals 4. This is caused by the power contributions from generators reacting to the frequency deviation. This corresponds to the findings and examination of oscillations done in [12].

For the derivative controlled model, power output was reduced to 0 MW prematurely without a time delay because of these oscillations. As seen in Figure 6.5, most oscillations are observed after a few seconds of the unit trip. A time delay t_{delay} of a few seconds was therefore introduced to ensure power output is not reduced prematurely. In future work, another solution rather than a simple time delay, perhaps a filter, should be developed in order for the model to work in power systems with larger oscillations.

In this study, the initial frequency signal is not passed through a filter in either model. Time and difficulty applying such a filter are reasons why it was not implemented. Also, frequency in the model of the Nordic grid in PSS/E does not suffer from small, quick frequency changes that often occur in a real power system, and therefore there is no need for a filter.

6.2.3 Additional Control

Both droop control and derivative control models determine resulting power output. Additional control in the form of limitations and characteristics of BESS are then

included in both models. The subsequent control of both models is illustrated in Figure 6.6.

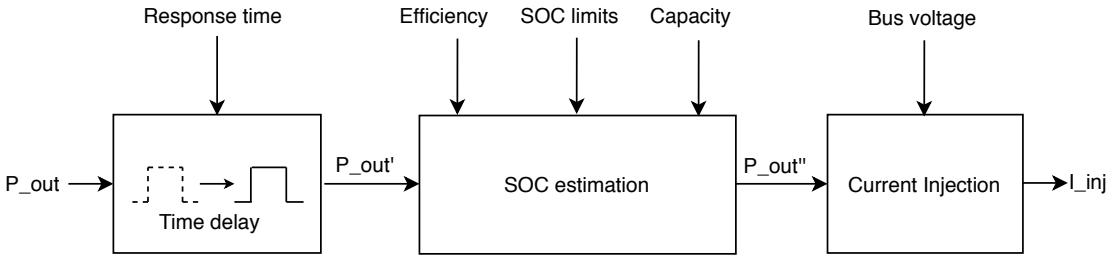

Figure 6.6: Block diagram showing additional control blocks of the two BESS models. The P_{out} signal is delayed by the response time resulting in P'_{out} which is the deylayed signal. Efficiency, SOC limits and capacity are used in the SOC estimation resulting in P''_{out}. The bus voltage is then used to calculate the current injection I_{inj}.

Response time of BESS is considered as the response of a PCS system is not instantaneous [62]. As illustrated in Figure 6.6, response time is introduced as a time delay, which can be varied depending on the actual response of the PCS. Per [66], for all battery storage technologies considered in this thesis response time is less than 1/4 cycle in a 60 Hz power system. In [62], the response time for a lithium-ion BESS is tested. From rest to full power output, the measured response time is found to be roughly 8.3 ms.

As explained in subsection 4.2.6, controlling SOC is crucial for overall operation of BESS. It must be controlled so that the BESS can provide the intended frequency support and SOC limits must be considered to maintain operational capacity, safety and limit aging. This is done in the SOC estimation block shown in Figure 6.6.

There are a few different ways to determine the SOC of batteries and the method used in this thesis is referred to as Coulomb Counting [62]. It is based on estimating the remaining capacity of the battery depending on charging or discharging rates. SOC at time t is calculated as

$$SOC(t) = SOC(t-\delta) - \frac{1}{E_b}\int_{t-\delta}^{t} \frac{P_{mech}}{\eta}\, dt \tag{6.1}$$

where δ is the time step between each sample, E_b is the energy rating of the battery in MWh and integration of $\frac{P_{mech}}{\eta}$ is the energy into or out of the battery in MWh. At t=0 SOC is equal to $SOC_{initial}$.

Round trip efficiency (η_{rt}) of BESS is the contribution of both charging efficiency (η_c) and discharge efficiency (η_d). To simplify modeling, it is assumed that charge and discharge efficiency is the same. This same assumption is used in studies [62], [67]-[70]. The efficiency (η) can therefore be obtained as

$$\eta = \eta_c = \eta_d = \sqrt{\eta_{rt}}\,. \tag{6.2}$$

Using the lowest round trip efficiency for lithium-ion of 90 % presented in Table 6.1, charge and discharge efficiency is obtained as roughly 95 %. The efficiency is used to calculate the energy drawn from the battery based on the power output.

The SOC limits SOC_{max} and SOC_{min} are used to limit charging or discharging beyond a certain threshold. In this study, full power output/input is allowed between 10-90 %. These limits were chosen because for lithium-ion batteries to maintain capacity, operational safety and to improve lifetime, full charge/discharge is usually limited to DOD at 80 % which corresponds to SOC between 10 - 90 % [31], [62]. If these limits are breached, P_{out} after the SOC estimation block in Figure 6.6 is reduced to 0.

6.3 Verification of BESS Models

The two developed models were tested to see if the designed controllers worked as intended. The test grid used is a simple three bus system with two generators, one load and one BESS, shown in Figure 6.7

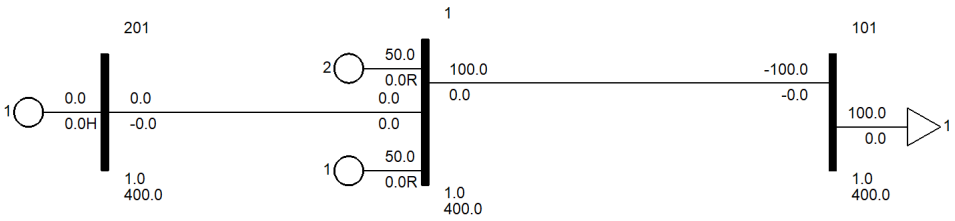

Figure 6.7: Test grid used to verify BESS models. Bus 1 is the swing bus with two generators producing 50 MW each, bus 101 has a load of 100 MW, and the BESS is installed at bus 201. The transmission lines are lossless and system voltage is 400 kV.

The generators at bus 1 in Figure 6.7 are modeled as hydro generators with the same dynamic models used in the model of the Nordic power system: GENSAL is used as generator model, SCRX as exciter, STAB1 as stabilizer, and WEHGOV is assigned as the turbine governor.

For the test case, initial condition with frequency regulated at 50 Hz is run for 10 seconds. At 10 seconds generator 2 at bus 1 is disconnected. This creates 50 MW generation deficit and a large frequency deviation. Dynamic simulations are then continued to see how the BESS at bus 201 reacts to the frequency deviation and how frequency stability is improved.

6.3.1 Droop Controlled Model Test

The values listed in Table 6.2 are assigned to the droop controlled model.

Table 6.2: Assigned values to the droop controlled model for test case.

Parameter	Value
Dead band limits	± 0.1 Hz
P_{max}	10 MW
Proportional gain K	-125
Efficiency η	95 %
Response time	0.083 ms
Initial SOC	50 %
SOC lower limit	10 %
SOC upper limit	90 %
Battery capacity	6.58 MWh

The values for dead band limits, proportional gain, efficiency and response time, listed in Table 6.2 and assigned to the model, are correlated to providing FCR-D with a BESS that has characteristics of lithium-ion battery technology. The SOC limits are set and capacity is calculated for the BESS to run at P_{max} for 15 minutes while maintaining acceptable SOC. The resulting frequency deviation and BESS power output is shown in Figure 6.8.

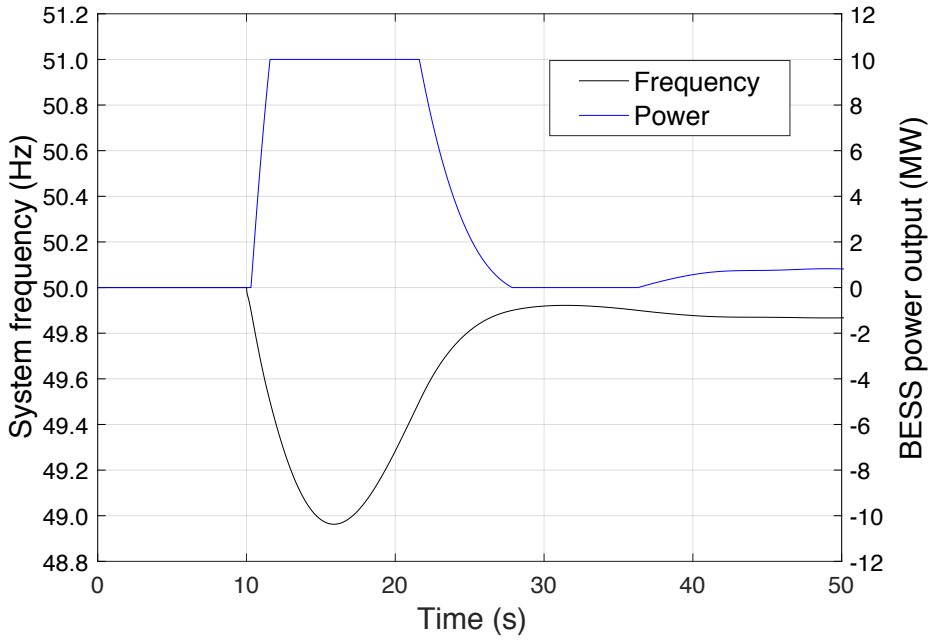

Figure 6.8: Frequency of the test grid and BESS power output with droop control. At 10 seconds a 50 MW generator is disconnected resulting in frequency deviation. When frequency drops below 49.9 Hz the BESS power output is increased.

As seen in Figure 6.8, the droop controlled model works as intended. When frequency drops below 49.9 Hz the power output of the BESS is increased in relation to the frequency deviation. Below 49.5 Hz BESS power output is at its maximum and when frequency is within 50 ± 0.1 Hz BESS power output is 0 MW.

A loss of load case was also tested. For this case, load was decreased at 10 seconds to 30 MW to demonstrate a large loss of load. The resulting frequency and power output is shown in Figure 6.9

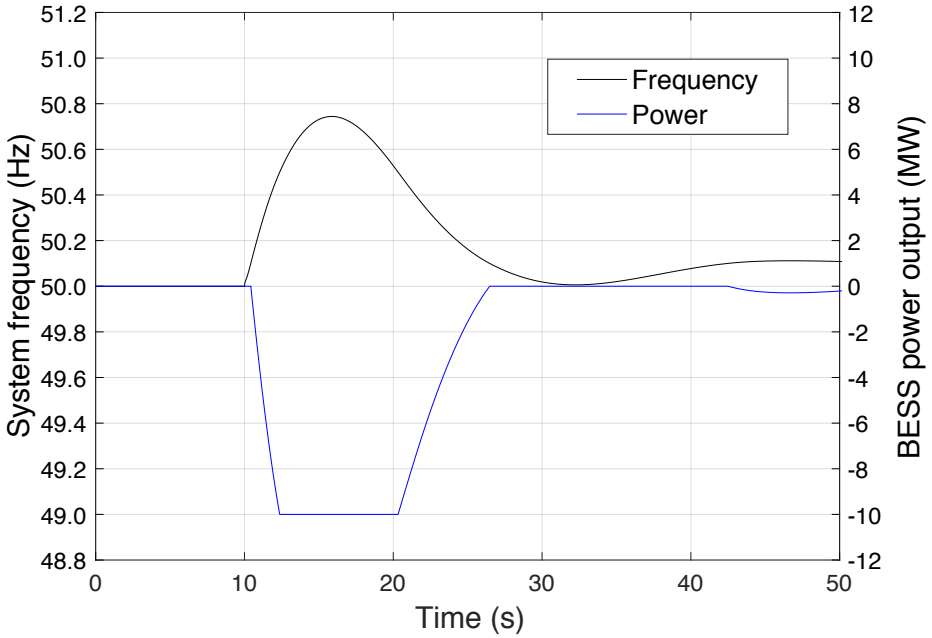

Figure 6.9: Frequency of the test grid and BESS power output with droop control for a loss of load. At 10 seconds the 100 MW load is decreased to 30 MW resulting in a positive frequency deviation from 50 Hz. When frequency is above 50.1 Hz the BESS power output is increased and it is at maximum at 50.5 Hz.

Figure 6.9 illustrates that the model also works for positive frequency deviations. Power is increased when frequency deviates beyond 50.1 Hz and reaches maximum power at 50.5 Hz.

Figure 6.10 shows the same response shown in Figure 6.8 of the droop control model for over 20 seconds. This is to compare the droop model with the derivative controlled model.

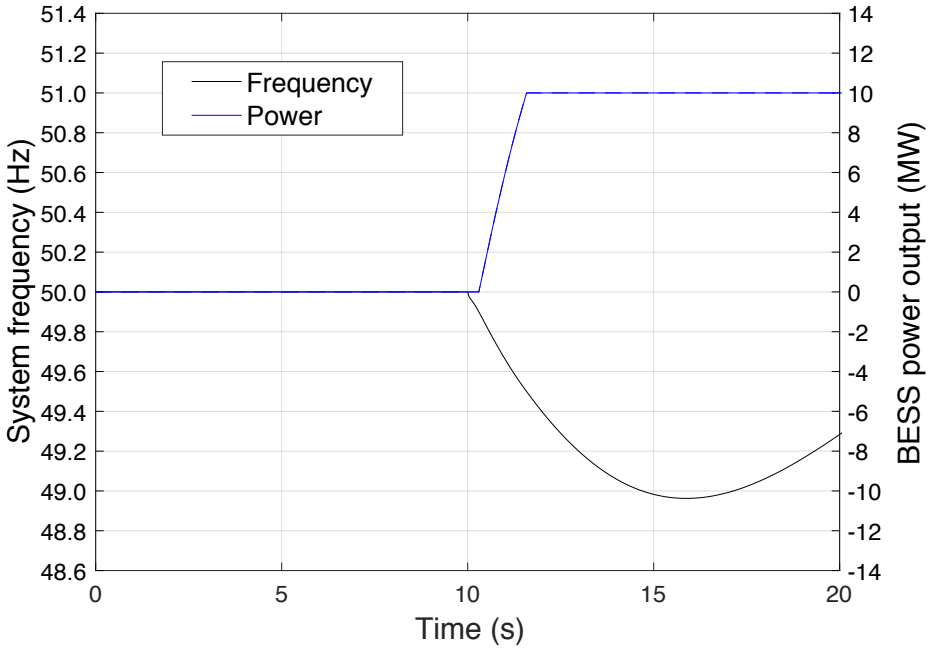

Figure 6.10: Frequency of the test grid and BESS power output with droop control for a loss of generation. At 10 seconds a 50 MW generator is disconnected resulting in frequency deviation. When frequency drops below 49.9 Hz the BESS power output is increased with maximum power output at 49.5 Hz.

6.3.2 Derivative Controlled Model Test

Values listed in Table 6.3 are assigned to the RoCoF controlled model for the same test case used in testing the droop controlled model with 50 MW production loss at 10 seconds in the simple 3-bus system.

Table 6.3: Assigned values to RoCoF controlled model for the test case.

Parameter	**Value**
Dead band limits	± 0.19 Hz/s
P_{max}	10 MW
Proportional gain K_{IR}	-5
Efficiency η	95 %
Response time	0.083 ms
Initial SOC	50 %
SOC lower limit	10 %
SOC upper limit	90 %
Battery capacity	6.58 MWh
t_{delay}	1 sec

The frequency deviation in the test case is large and therefore low proportional gain and high dead band limits should be assigned. This is to achieve the desired power response of the BESS, which is high initial contribution and gradual reduction in power output before frequency nadir is reached. The same SOC limits and battery

capacity are used as in droop model testing. For this test case, there are no large oscillations and premature power reduction is not possible and therefore t_{delay} is set at 1 second.

The resulting power output and frequency is shown in Figure 6.11.

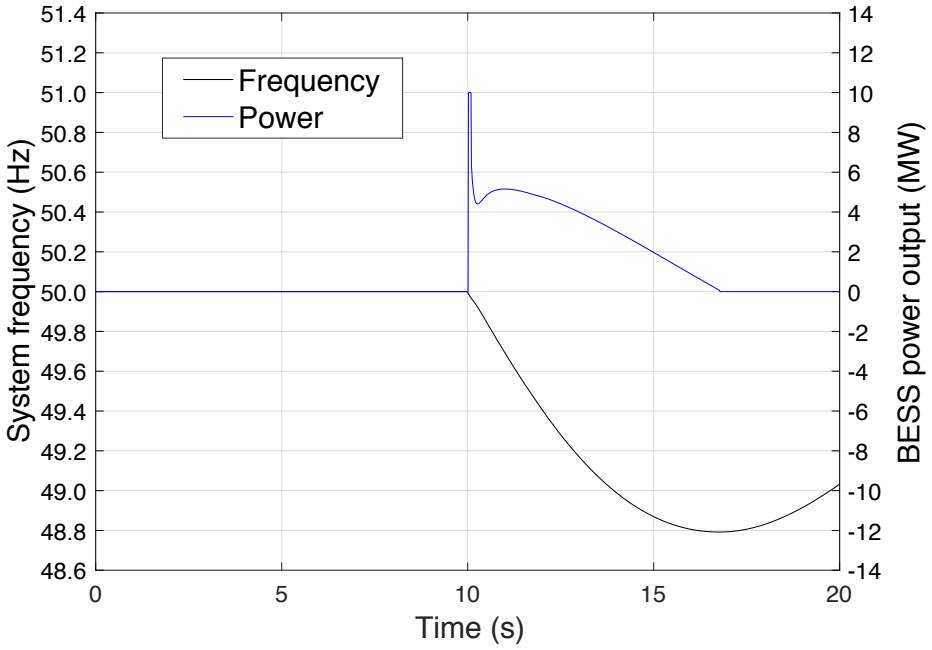

Figure 6.11: Frequency of the test grid and BESS power output with RoCoF control. At 10 seconds a 50 MW generator is disconnected and almost instantaneously BESS output is regulated to counter the resulting in frequency deviation. When frequency reaches point of minimum frequency power output is reduced to 0 MW.

As seen in Figure 6.11 the derivative controlled model works as intended. When the 50 MW production unit is disconnected at 10 seconds, frequency rapidly decreases. The BESS reacts to this frequency deviation and increases its power output.

The initial variations in power output seen in Figure 6.11, might seem unexpected but it is anticipated. Based on observations made in section 5.5, frequency does not behave as expected for about half a second after a major frequency event in PSS/E. The sudden surge in power from the BESS also contributes to variations in frequency.

6.3.3 State of Charge Test

To verify that the SOC estimation works as intended a SOC test was conducted. The BESS discharge duration in seconds before the lower SOC limit is breached can be calculated using

$$\frac{E_{BESS} \cdot (SOC_{initial} - SOC_{min}) \cdot \eta}{P_{BESS}} \cdot 3600 \tag{6.3}$$

where E_{BESS} is the capacity in MWh, $SOC_{initial}$ is the initial SOC level, SOC_{min} is the lower SOC level, η the discharge efficiency, and P_{BESS} power output. For a droop controlled BESS running at power output P_{BESSS} 10 MW, with battery capacity E_{BESS} of 3 MWh, efficiency η of 95 %, initial SOC at 50 % and lower SOC limit at 49 %, the battery should be able to run for about 10.3 seconds for a large frequency deviation.

For this test case, proportional gain is increased to -900 and at 10 seconds generator 2 is disconnected and load is set to 500 MW, to ensure the BESS power output is at P_{max} for the duration of the test. The resulting BESS power output and frequency is shown in Figure 6.12.

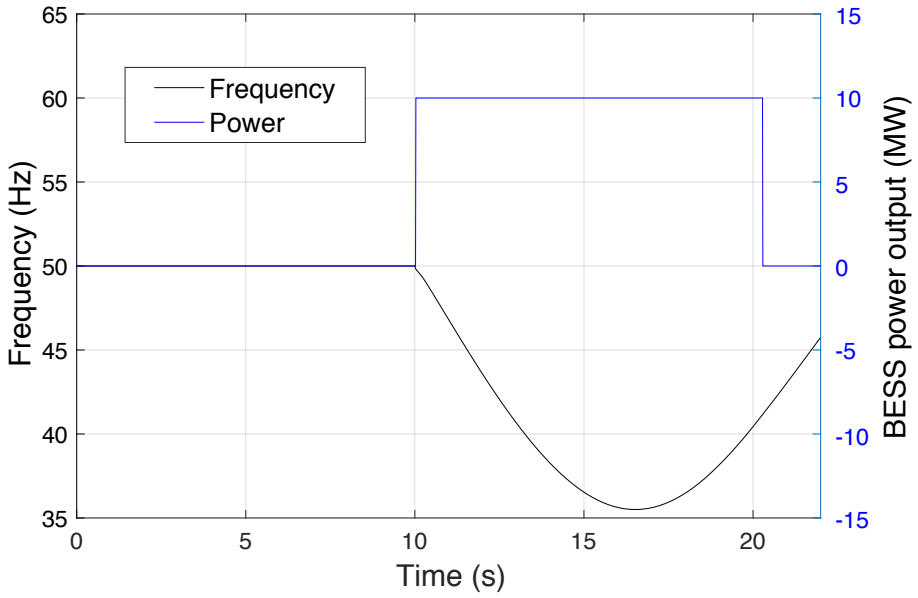

Figure 6.12: BESS power output and frequency to illustrate the function of the SOC estimation block. At 10 seconds one generator is disconnected and load is increased resulting in a large frequency deviation. As calculated BESS output is restricted after roughly 10.3 seconds of operation at full output.

As seen in Figure 6.12, at 10 seconds BESS power output is increased to maximum in response to the large frequency deviation, which is the result of disconnecting a generator and increasing load. As calculated, power output is restricted after roughly 10.3 seconds of running time when SOC is reduced from 50 % to 49 %.

7

Simulations using Modeled Grid with Battery Storage

Battery storage systems were integrated in the Swedish transmission system model in PSS/E and several simulations were run. These simulations are used to illustrate the potential of BESS in providing either primary frequency regulation or inertial response in the power system.

7.1 Simulation Studies

The simulation studies are:

1. Derivative controlled BESS with 0, 40, 100, 540 MW total power capacity.
2. Droop controlled BESS with 0, 40, 100, 540 MW total power capacity.
3. Single 540 MW derivative controlled BESS.
4. Single 540 MW droop controlled BESS.
5. 540 MW total BESS power capacity with in a system with reduced inertia and kinetic energy of 130 000 MWs.

The first two simulation studies, 1 and 2, are chosen to illustrate the improvement in system frequency stability with three different levels of BESS capacity in the system, using two control methods. The control methods designed in section 6.2 are applied, where derivative control is to provide inertial response and droop control is equivalent to provide FCR-D.

In simulation studies 1 and 2 the BESS power capacity is distributed over 11 units. Simulation studies 3 and 4 were chosen to illustrate the difference when using one large single unit instead of 11 units. Simulation study 5 shows the result of using 11 BESS with 540 total power capacity in a system with lower kinetic energy and how this is equivalent to providing kinetic energy.

The frequency at the swing bus located in market area SE2 is used to represent the system frequency as it is located relatively far away from the fault. The frequency at the Ringhals bus where Ringhals 4 is disconnected is the local bus frequency.

When using a single unit, it is installed at the bus where Ringhals 4 is disconnected. When 11 units are used, they are installed at different buses in the system. These are distributed in the model of Sweden roughly in relation to the production

in the Swedish market areas for the reference hour. The production distribution in market areas SE1-SE4 and distribution of BESS capacity is shown in Table 7.1.

Table 7.1: Distribution of production in market areas SE1-SE4 for the reference case, and distribution of BESS capacity in percentage of the total power capacity.

Area	**Production [MW]**	**BESS capacity [%]**
SE1	3 821	20
SE2	6 667	30
SE3	10 313	45
SE4	764	5
Sweden	21 457	100

Transmission capacity was considered when distributing the units by connecting BESS to buses with enough capacity to handle the additional power contribution.

The reference case of production hour 10:00-11:00 on 05 March 2015 with loss of Ringhals 4 (1110 MW), is used for all simulations. The kinetic energy for this case is estimated to 260 000 MWs. This load case was chosen as it provides a reference frequency response and the model was tuned and verified to this response of the Nordic power system, as explained in detail in section 5.4. The system frequency is observed from the swing bus located in SE2 and the local bus frequency is frequency at the Ringhals bus located in SE3.

Four levels of total installed BESS capacity were used: 0 MW, 40 MW, 100 MW and 540 MW. 0 MW is referred to as the Base case, which is the system response without installed BESS capacity. 40 MW was chosen as there are several battery storage units with 40 MW power rating installed globally and therefore this is deemed to be a feasible power rating for installation in Sweden. 100 MW was chosen as it is the power rating of the largest installed BESS to date. 540 MW is roughly the power rating needed in the system with 130 000 MWs kinetic energy E_k to achieve the same rate of change of frequency as in the system with 260 000 MWs kinetic energy. This was calculated from the swing equation using

$$P_{BESS} = \Delta P - \frac{\frac{df260}{dt} \cdot 2 \cdot E_k}{f_0} \tag{7.1}$$

where P_{BESS} is the BESS power output in MW, and $\frac{df260}{dt}$ is the RoCoF for the 260 000 MWs system.

7.2 Simulation Results

This section is divided into subsections corresponding to each simulation study to facilitate comprehension of the results.

7.2.1 Simulation Study 1

The resulting system frequency for the first simulation study is shown in Figure 7.1. In study 1, derivative controlled BESS are used with 0, 40, 100 and 540 MW installed capacity. The system frequency is monitored from the swing bus. Ringhals 4 is disconnected at 10 seconds and simulation is run for another 40 seconds.

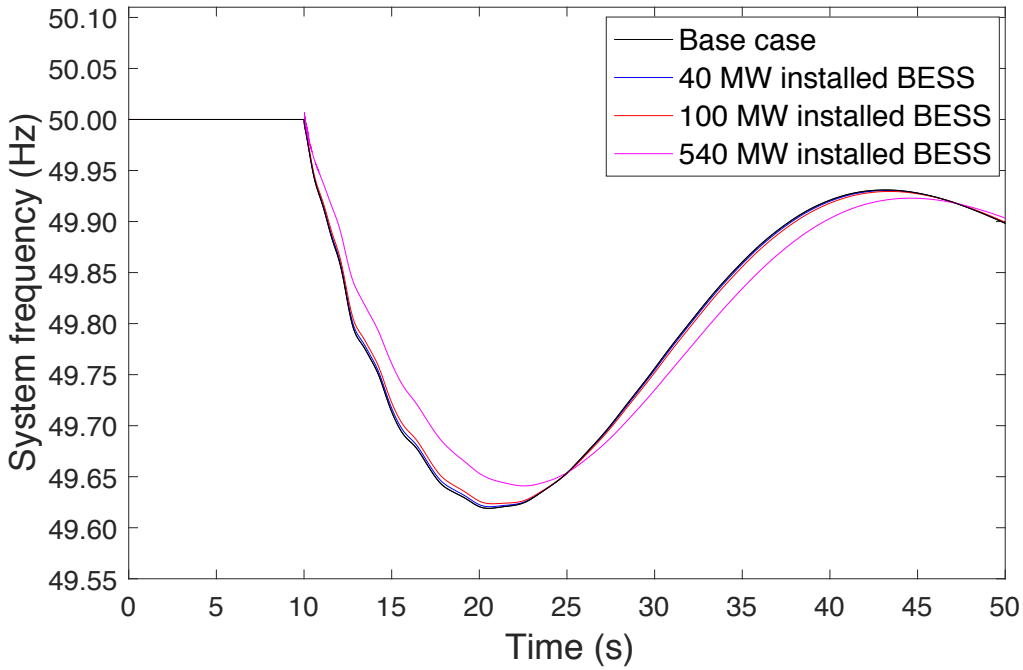

Figure 7.1: Simulation 1, with derivative controlled BESS of 0, 40, 100 and 540 MW capacity and monitoring system frequency from the swing bus. For 40 MW and 100 MW the change in frequency stability is very small. 540 MW installed capacity has a larger impact by raising and delaying time to nadir.

As seen in Figure 7.1 increasing BESS capacity from 0 to 540 MW decreases RoCoF and improves frequency stability. With 40 and 100 MW installed BESS the improvement in frequency stability is minimal. With 540 MW installed BESS capacity, frequency nadir is raised from 49.62 Hz to 49.64 Hz and time to nadir is delayed by 2 seconds. A temporary increase in frequency is seen at around 10 seconds, which is the result of the 540 MW BESS power contribution.

The local bus frequency is shown in Figure 7.2 and total BESS power output for this simulation study is shown in Figure 7.3.

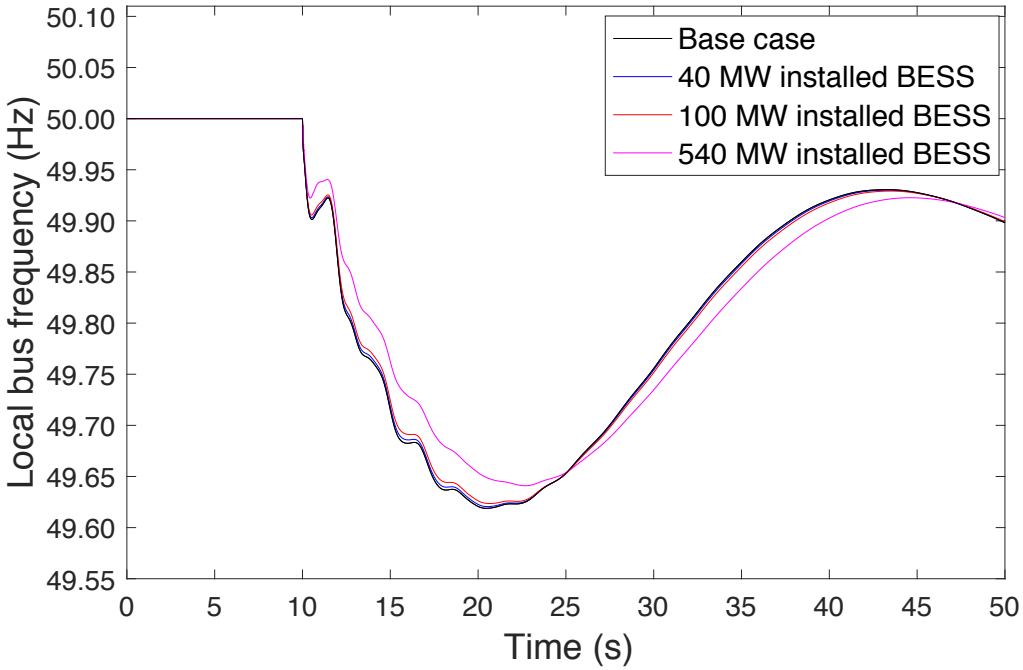

Figure 7.2: Simulation 1 with derivative controlled BESS of 40, 100 and 540 MW capacity. Monitoring the Ringhals bus frequency.

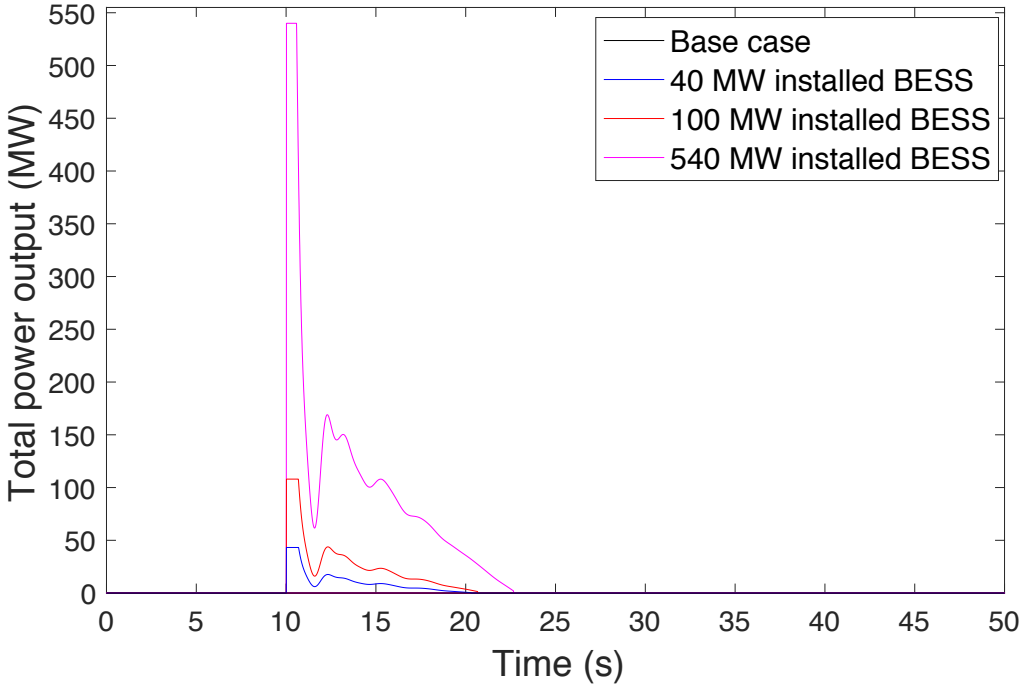

Figure 7.3: Simulation 1 with derivative controlled BESS of 40, 100 and 540 MW capacity. Monitoring the total BESS power output.

Similar results as shown in Figure 7.1 are seen in Figure 7.2 at the bus where the frequency event occurs, denoted the local bus. As seen in Figure 7.3 power output is increased to maximum, when RoCoF is largest. Oscillations in local bus frequency

caused by the large production loss result in power output variations. This is most notable at around 11-12 seconds where the temporary frequency increase results in a large decrease in BESS power output.

Consequently, from what is seen in Figure 7.1 and 7.2, very large BESS capacity is needed to improve frequency stability if BESS are used to provide inertial response. The most significant change seen when using inertial response is delaying time to nadir. Only minor improvements in frequency deviations are seen but this is as expected from the observations made in section 5.5, where substantial reduction in inertia only slightly reduced frequency nadir. Large capacity could also introduce unwanted frequency spikes when the system experiences sudden surges of power from BESS as seen in Figure 7.1.

7.2.2 Simulation Study 2

The result of simulation study 2 is shown in Figure 7.4, where system frequency is observed. Droop control is used for the 11 BESS units with 0, 40, 100 and 540 MW installed power capacity and the system frequency is monitored from the swing bus. At 10 seconds Ringhals 4 is disconnected and simulation is then run for another 40 seconds.

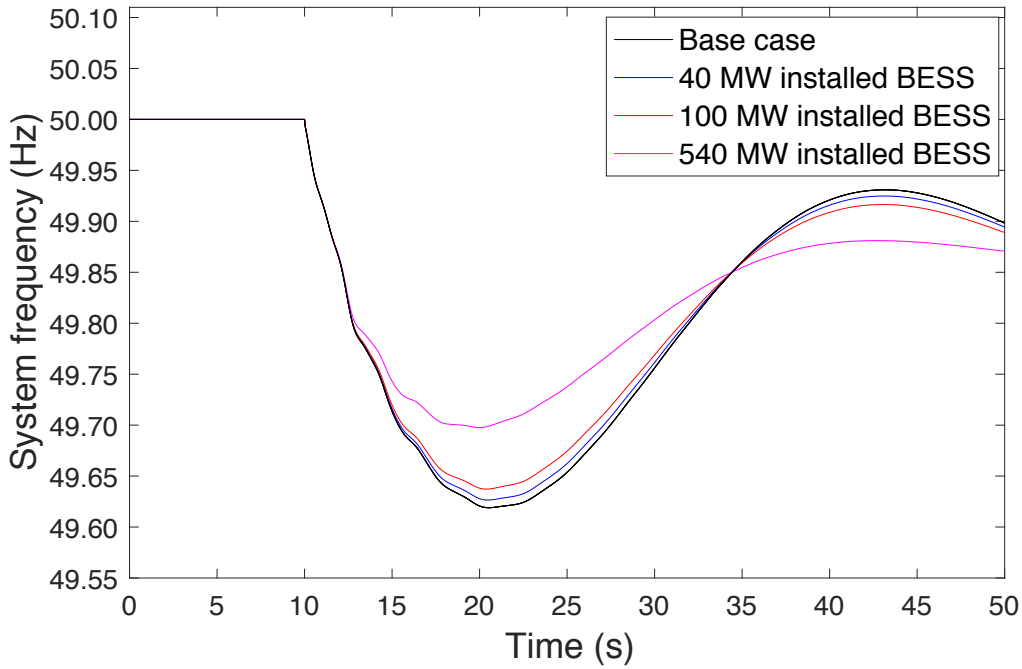

Figure 7.4: Simulation 2 with droop controlled BESS of 40, 100 and 540 MW capacity. With increased capacity frequency deviation is reduced.

As illustrated in Figure 7.4, increasing BESS capacity notably improves frequency stability by raising nadir. It also decreases following oscillations in frequency as seen in the figure at around 40-45 seconds. There are however no significant improvements in RoCoF and time to nadir is slightly reduced.

The local bus frequency and total BESS power output for this simulation study is shown in Figure 7.5 and .

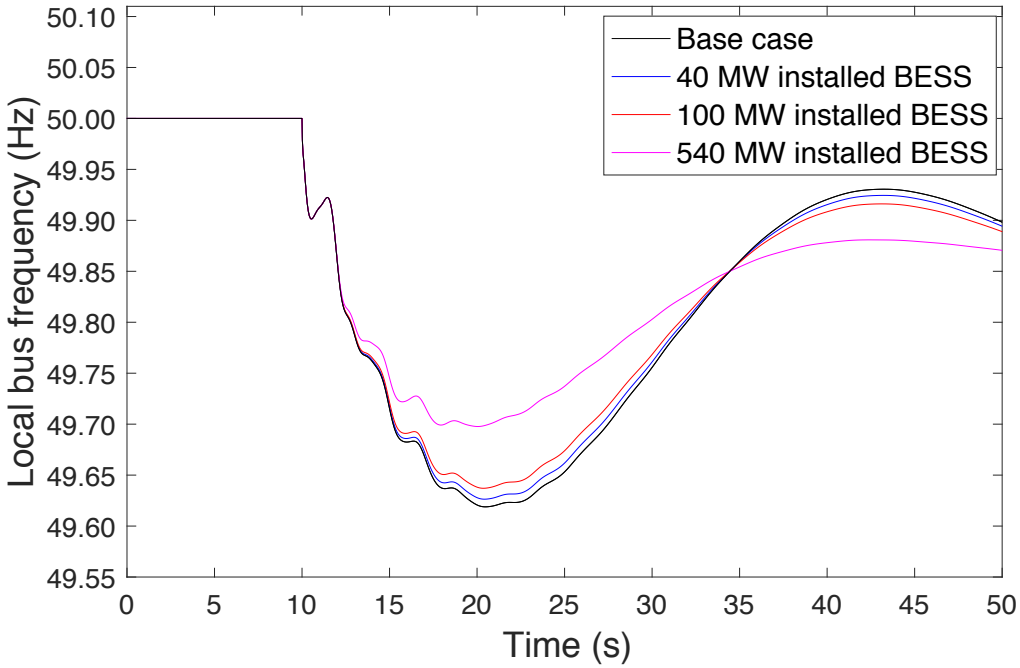

Figure 7.5: Simulation 2 with droop controlled BESS of 40, 100 and 540 MW capacity. Monitoring the Ringhals bus frequency. With increased capacity frequency deviation is reduced.

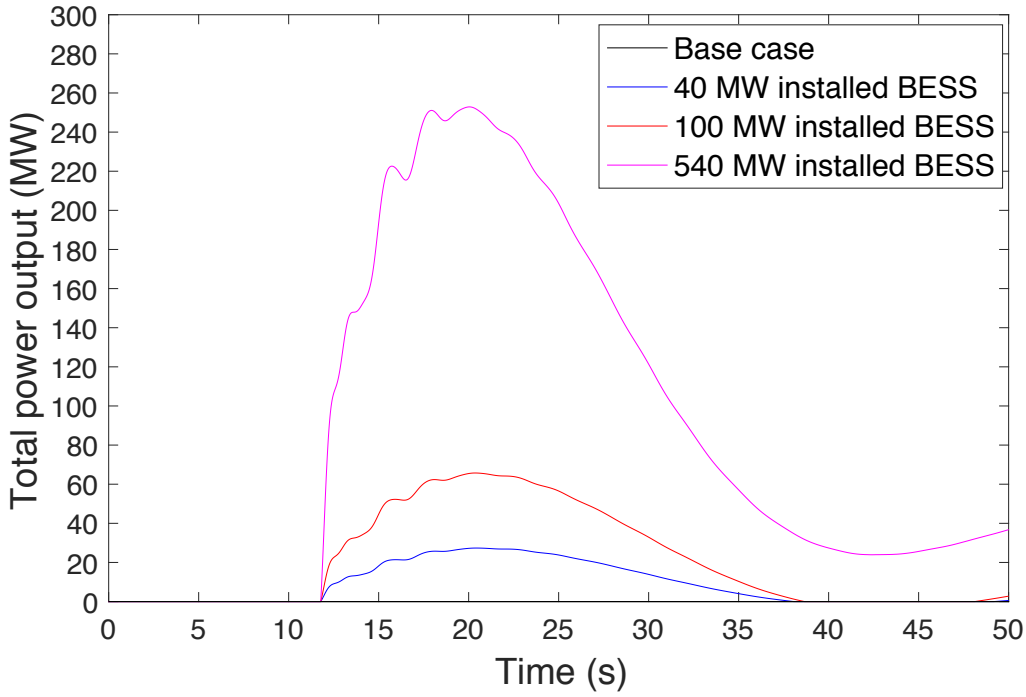

Figure 7.6: Simulation 2 with droop controlled BESS of 40, 100 and 540 MW capacity. Monitoring the total BESS power output. Total power output does not reach maximum capacity as frequency deviation does not drop to 49.5 Hz.

As seen in Figure 7.5 and 7.6, when frequency drops below 49.9 Hz at around 12 seconds power output increases. Frequency never drops below 49.5 Hz and therefore power output does not reach full output capacity. It is closet for 40 MW installed capacity, which reaches almost 30 MW. For both the 100 MW and 40 MW cases power output is reduced to 0 MW at roughly 38-39 seconds as frequency is above 49.9 Hz.

Compared to derivative control, droop control is superior in reducing frequency deviations. Even for 40 MW installed capacity there is a notable different in frequency deviation. There are no sudden power surges and therefore the system does not experience rapid changes in frequency and following oscillations before frequency settles at steady state frequency are also reduced.

7.2.3 Simulation Study 3

The result of the third simulation study is shown in Figure 7.7 and 7.8. A single 540 MW BESS unit is installed at the Ringhals bus and derivative control is implemented.

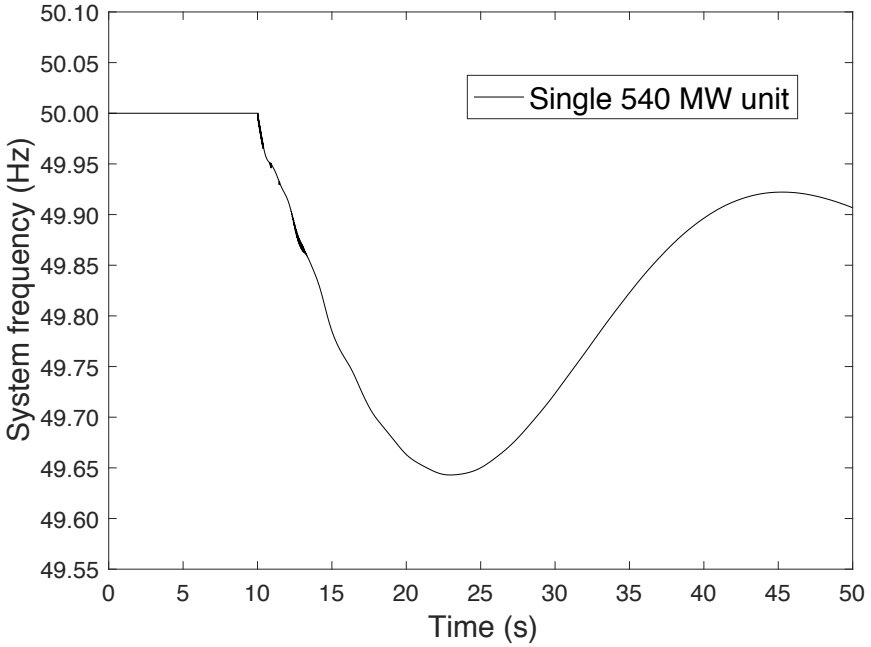

Figure 7.7: Simulation 3 with a single derivative controlled BESS of 540 MW power capacity, showing the system frequency.

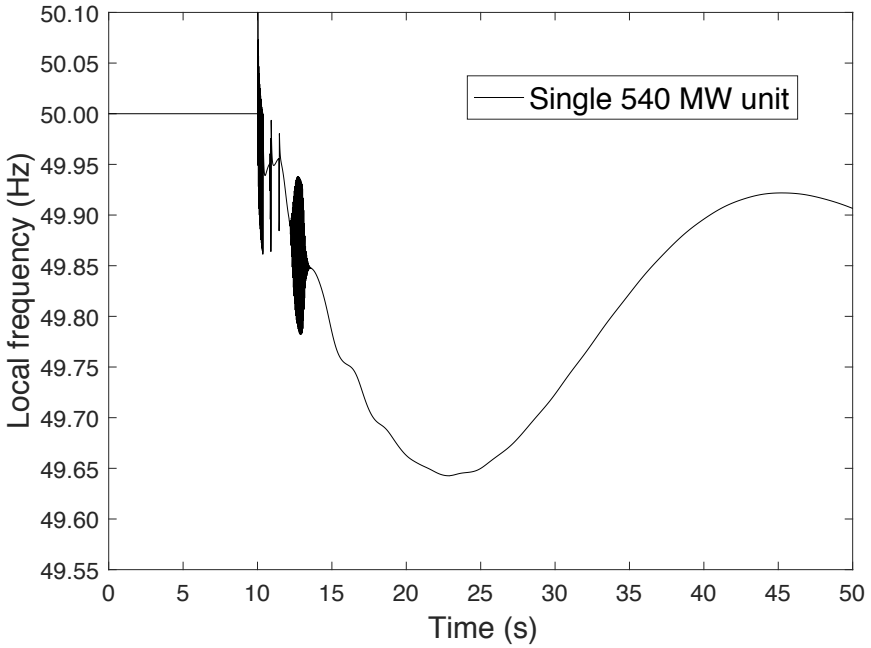

Figure 7.8: Simulation 3 with a single derivative controlled BESS of 540 MW power capacity, showing the Ringhals bus frequency.

As seen in Figure 7.7 and 7.8, having a single unit with 540 MW power rating results in major frequency distortion at the local bus. This is the result of the large changes in power output, which could cause major implications for the power system.

The Ringhals bus frequency and BESS power output between 9.9 and 10.5 seconds are shown in Figure 7.9 and 7.10.

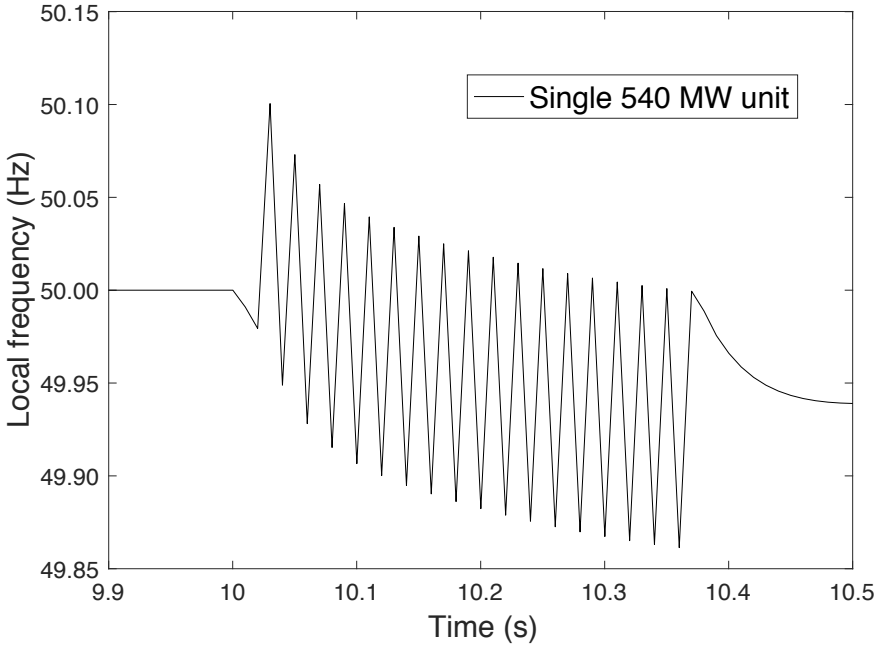

Figure 7.9: Simulation 3 with a single derivative controlled BESS of 540 MW power capacity, showing the Ringhals bus frequency between 9.9 and 10.5 seconds.

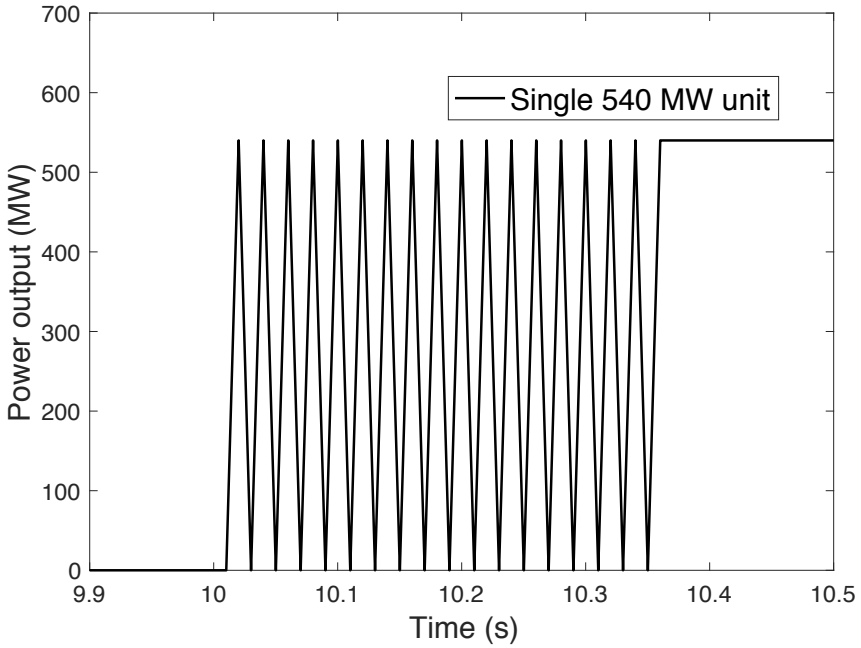

Figure 7.10: Simulation 3 with a single derivative controlled BESS of 540 MW power capacity, showing the BESS power output between 9.9 and 10.5 seconds.

Seen in Figure 7.9 and 7.10 is that power output is increased to maximum when

frequency deviates because of the loss of Ringhals 4. This in turn increases frequency and thus power output is reduced. This causes the deviations seen in Figure 7.7 and 7.8.

7.2.4 Simulation Study 4

In simulation study 4, a single droop controlled BESS with 540 MW capacity is installed. The resulting system frequency and Ringhals bus frequency deviations are shown in Figure 7.11 and 7.12.

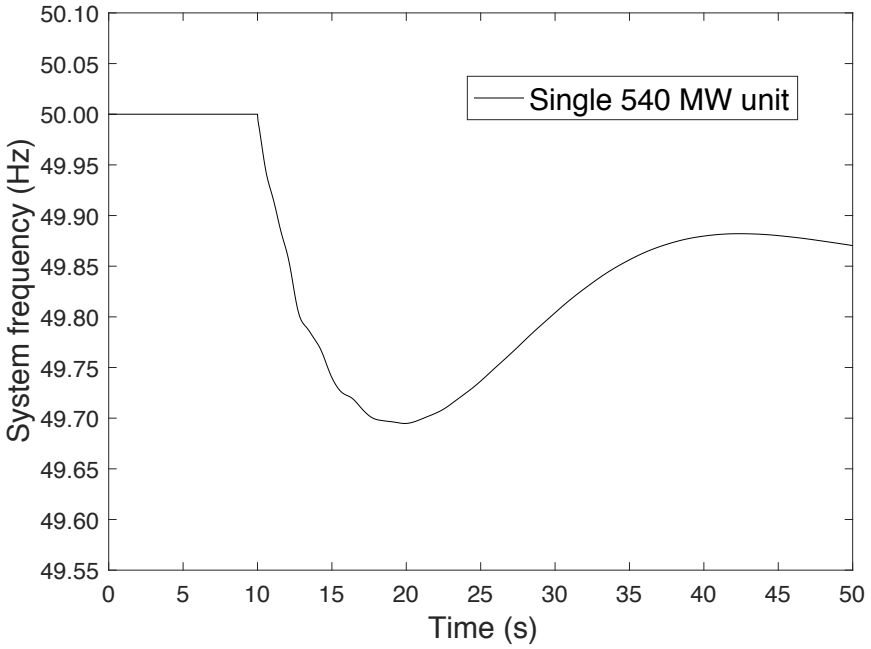

Figure 7.11: Simulation 4 with a single droop controlled BESS of 540 MW power capacity showing the system frequency.

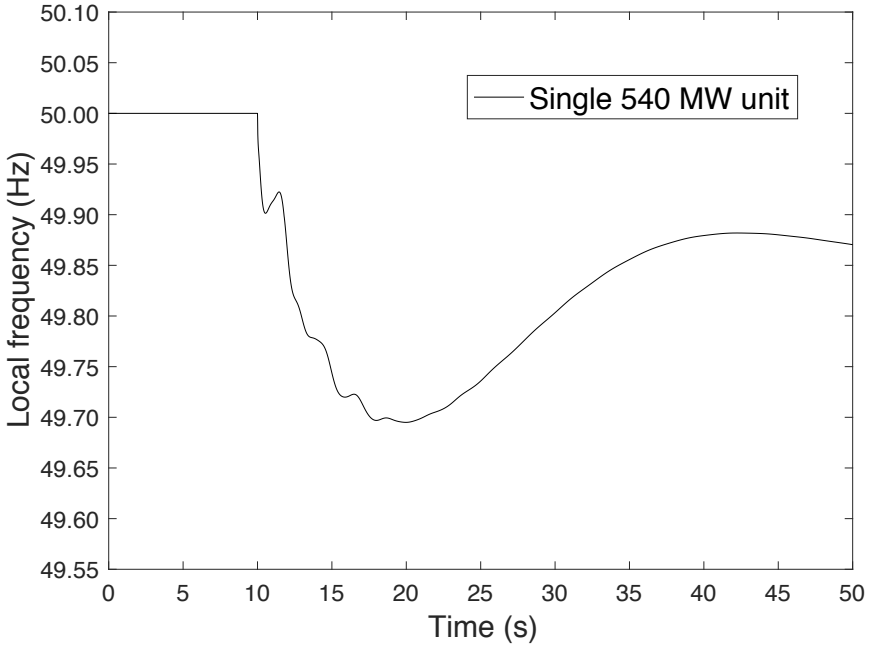

Figure 7.12: Simulation 4 with a single droop controlled BESS of 540 MW power capacity showing the Ringhals bus frequency.

As seen in Figure 7.11 and 7.12, with a single droop controlled BESS of 540 MW power capacity there is no noticeable distortion in frequency at the system or local bus. There is also no noticeable difference when using 11 distributed droop controlled units compared to using a single droop controlled unit when comparing the results shown in Figure 7.4, 7.5 and Figure 7.11 and 7.12, illustrated in Figure 7.13 and 7.14.

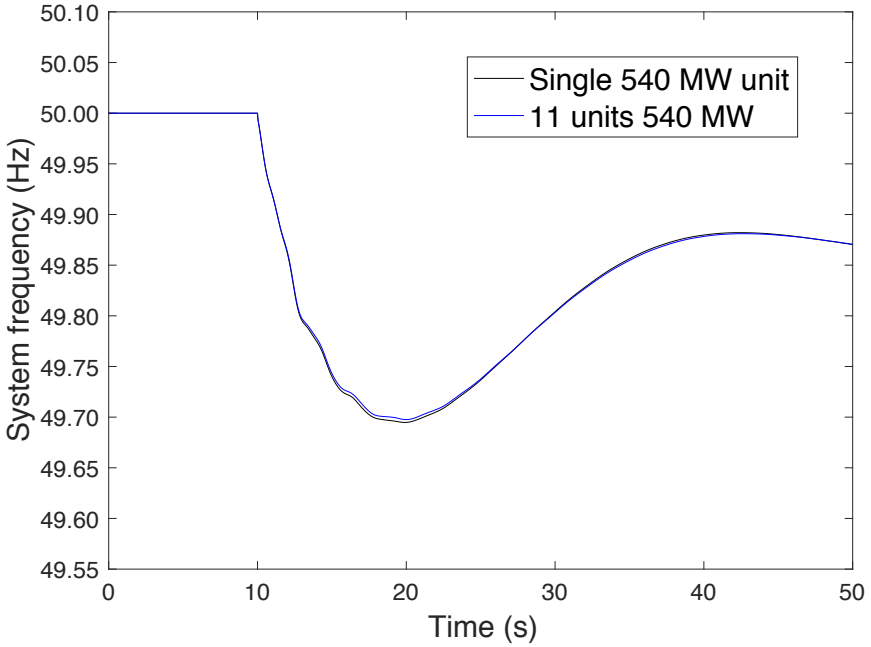

Figure 7.13: A single droop controlled BESS of 540 MW power capacity compared to 11 units with 540 MW total power capacity, showing system frequency.

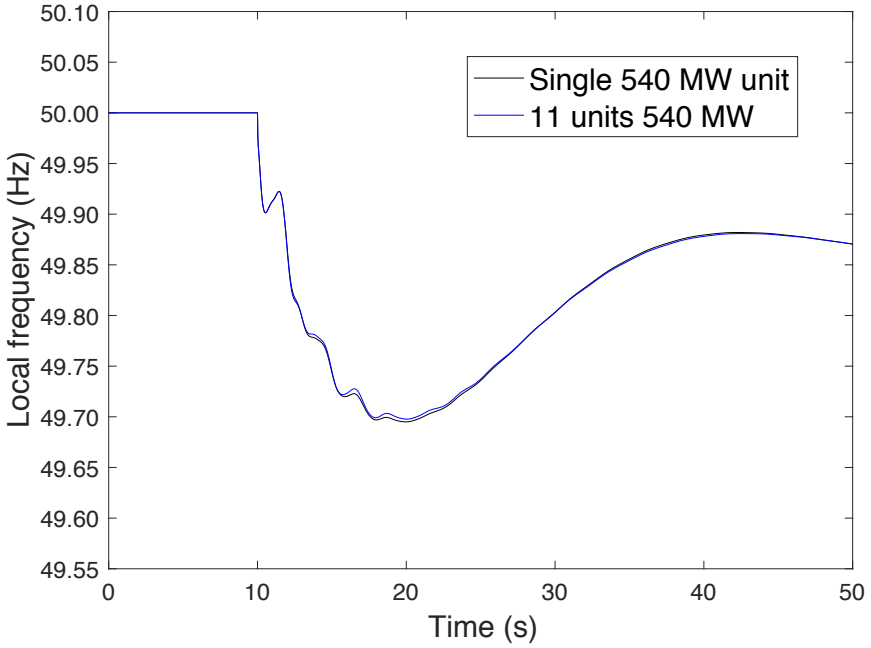

Figure 7.14: A single droop controlled BESS of 540 MW power capacity compared to 11 units with 540 MW total power capacity, showing Ringhals bus frequency.

However, because of what is seen in Figure 7.8, where frequency is seriously distorted because of the large power contribution from the single 540 MW BESS, capacity was distributed over 11 units for simulations 1 and 2 for both droop and derivative control cases. This was to have the same initial conditions for all cases and to avoid power

and frequency instabilities in the power system when using derivative control.

7.2.5 Simulation Study 5

Three cases are included in this study. First the base case, which is the system without BESS and 260 000 MWs kinetic energy. Secondly the system with 130 000 MWs kinetic energy. Third and last, the system with 130 000 MWs kinetic energy and 540 MW derivative controlled BESS. The system frequencies for these three cases are shown in Figure 7.15.

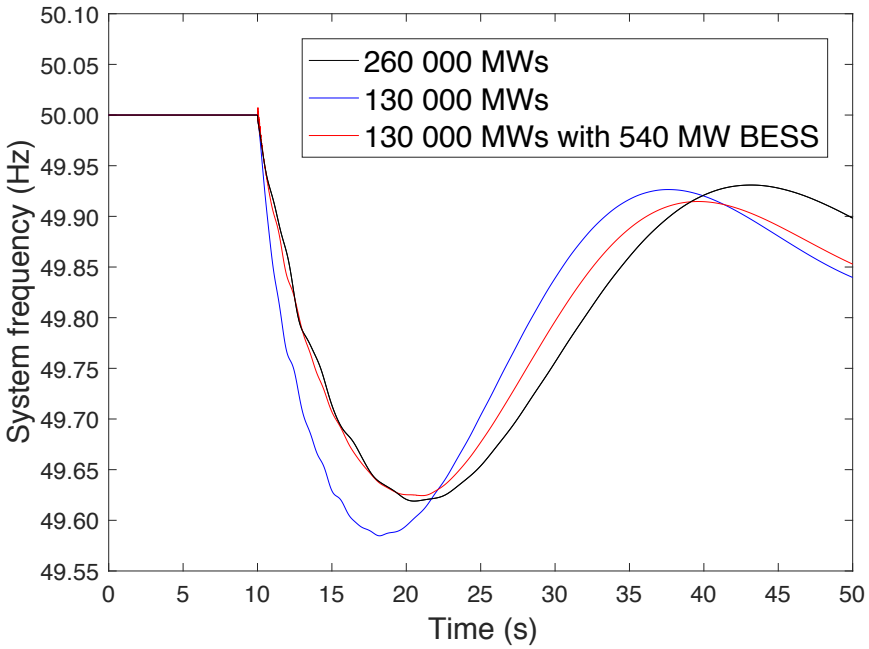

Figure 7.15: System frequency for three cases: system with 260 000 MWs kinetic energy, system with 130 000 MWs kinetic energy, and system with 130 000 MWs kinetic energy with 540 MW BESS capacity.

As seen in Figure 7.15, reducing kinetic energy from 260 000 MWs to 130 000 MWs causes larger frequency deviation because of increased rate of change of frequency. With a 540 MW derivative controlled BESS in the 130 000 MWs system, RoCoF is reduced to a similar level of the 260 000 MWs system. Frequency nadir is increased and time to nadir is delayed. A temporary increase in frequency is seen after 10 seconds, which is also seen in Figure 7.1 for large derivative controlled BESS capacity.

The difference in slope after frequency nadir can be explained by how the derivative controlled model was designed. Real inertial response from the power system has both a positive and negative contribution following a production loss, which is seen in Figure 3.2 and in the ENTSOE report [12]. Once frequency nadir has been reached, real inertial response goes from positive to negative as rotating synchronous machines begin to accelerate, explained in subsection 3.2.1 and in [12]. This behavior is not included in the BESS derivative controlled model as this aggravates the

frequency stability situation. Instead power output is reduced to 0 MW when frequency nadir is reached. As seen in Figure 7.15, this has a positive impact on the power system.

7.3 Economic and Lifetime Analysis

The following simple economic and lifetime estimations are used to illustrate the cost of installing BESS in the Swedish power system, the potential income that could be made and the possible lifetime of a lithium-ion BESS for this application. Several estimations and assumptions are made and therefore the outcome of this section should only be interpreted as an indication of the possible outcome. Only FCR-D is considered since there is currently no market for providing inertial response in the Nordic power system.

The characteristics of the lithium-ion battery system used in these estimations are from Table 6.1. Efficiency is assumed to be 0.95 %, SOC limits are at 10 and 90 %, and initial SOC is kept at 50 %. In most battery applications, a battery is deemed to have reached its full lifetime when capacity is reduced to 80 % [31]. Consequently, calculated battery capacity will be increased by 20 %, to compensate for this loss of capacity. Based on the current requirements on FCR-D in the Nordic power system, the required BESS capacity E_{BESS} for different desired MW power outputs P_{BESS} can be calculated using

$$E_{BESS} = \frac{P_{BESS} \cdot t_d}{(SOC_{initial} - SOC_{limit}) \cdot \eta \cdot 0.8} \tag{7.2}$$

where t_d is the required power duration, $SOC_{initial} - SOC_{limit}$ is the depth of charge or discharge. For the calculations t_d is 0.25 hours, $SOC_{initial} - SOC_{limit}$ is 0.4, η is 0.95, and divided by 0.8 to compensate for the capacity loss.

Using capacity cost of 10 million SEK/MWh from Table 6.1, the resulting estimated capacities needed and cost of 40, 100 and 540 MW BESS power output are shown in Table 7.2.

Table 7.2: BESS capacity needed and cost of BESS in the Nordic power system to supply FCR-D.

Power output	Capacity	Cost
40 MW	33 MWh	330 million SEK
100 MW	82 MWh	820 million SEK
540 MW	444 MWh	4440 million SEK

The potential income is calculated using the yearly price for FCR-D during 2017. Based on historical data of average hourly price for FCR-D in SEK/MW from [71], the yearly price is 630 000 SEK/MWyear. FCR-D is procured through pay-as-bid and therefore the average price is assumed [72]. If this yearly price is given every

year the BESS is active, the expected income per desired power output, is as shown in Table 7.3.

Table 7.3: BESS capacity profit per year based on total price for FCR-D during 2017 from [71].

Power output	Profit
40 MW	25 million SEK/year
100 MW	63 million SEK/year
540 MW	340 million SEK/year

If the estimation of income shown in Table 7.3 is calculated as profit, each BESS must be operational for more than 13 years in order to cover the initial costs. But this is assuming the BESS is operational for every hour, there are no operation and maintenance costs, calendar aging is assumed to have no effect, and the most implausible assumption is that FCR-D for down regulation is followed directly by FCR-D for up regulation, to cover charging of a BESS following a discharge.

Lifetime of a BESS can be measured in both years and cycles. The current maximum expected lifetime measured in years for a general lithium-ion BESS is 15 years and the expected cycle life is 1000-10 000 cycles, which is a wide range without specified DOD or discharge/charge current [5], [9], [10]. The expected cycle lifetime can instead be estimated based on the results found in [31] and [73]. For the intended operation with 40 % DOD at initial SOC at 50 %, 4C discharge current, and assuming low operating temperature at 25^o C, the expected cycle lifetime is estimated to roughly 3000 cycles.

In [1] an estimation of the number of minutes per week frequency is outside 50 $\pm$ 0.1 Hz is presented. The trend seen over the last 15 years is increasing frequency deviations and at the end of 2016 the average was at 250 minutes per week, which is 13 000 minutes per year [1]. For the BESS assumed in this chapter, a discharge and charge cycle at full power rating would take roughly 72 minutes. With the estimation of frequency deviations for 13 000 minutes per year the BESS would be going through roughly 180 full cycles per year. With 180 cycles per year and 3000 cycles for its full lifetime, the battery could last approximately 16 years.

The economic and lifetime analysis and estimations conducted in this section illustrate the challenges involved with the application lithium-ion battery storage in power system application. With 15-16 year lifetime, it is possible the battery could last the required minimum 13 years to cover installation costs, but this is with the very ambitious assumptions made. Either cost has to be reduced or another market has to be created for BESS to increase profits and reduce the capacity needed to fulfill the requirements. An alternative solution would be to use sodium-sulfur battery technology, which has lower cost and similar characteristics of lithium-ion batteries, with high efficiency and power density. However, significant development of sodium-sulfur technology is needed before this can be deemed a serious alternative to lithium-ion.

8
Discussion

8.1 Significant Findings

Based on the findings in section 7.2, BESS have the potential to improve frequency stability in the Nordic power system. However, the economic and lifetime estimations conducted in section 7.3 indicate the possibilities to profit from investing in BESS are currently severely limited. Even with exaggerated assumptions, the possibilities of BESS are restricted with the current market and requirements on FCR-D. The batteries must have extremely high capacity and will therefore be expensive, and even then, they risk not fulfilling the requirements. One reason being that they need time to charge following a discharge, which is not accounted for in the current regulations. With no economic incentives, large-scale deployment and installation of lithium-ion BESS for frequency control will not be realized.

The constant development of lithium-ion batteries is rapidly reducing the price and increasing lifetime which can enable the deployment in the future. However, incentives and new market services, such as the Enhanced Frequency Response used in Great Britain mentioned in subsection 3.2.5, should also be introduced to utilize the recognized potential of BESS. Alternatively, when sodium-sulfur BESS has been commercialized it could prove to be a cost effective alternative to lithium-ion with similar characteristics.

Worth mentioning again, presented in section 4.1, is that most BESS projects deployed in power systems around the world, have more than one operational application. If a BESS is to only provide support during frequency disturbances, the discharge current will be high and it will remain idle for long periods of time and this is not ideal for the operation of lithium-ion battery systems. The effects of calendar aging on capacity, shown in [31], would be one of many concerns. The recommendation would therefore be to investigate BESS applications that could complement the frequency control. An example of this being the Hornsdale power reserve project, where part of the BESS is dedicated to frequency control and part for load shifting [29]. With more than one application the total battery capacity can be increased and discharge current can be reduced, which could reduce the effects of aging resulting in a longer lifetime.

Another important finding illustrated in this thesis is the consequences of using a single large unit compared to using 11 smaller units. If the units are controlled

with no sudden power surges, as in the droop control when providing FCR-D illustrated in Figure 7.13 and 7.14, there are no significant differences. But when using the derivative controlled units, shown in Figures 7.7 and 7.8, there are serious oscillations when using a single large unit. This is important to consider as it has consequences for the potential deployment of BESS in the power system. Installation of several smaller units might be considered more realistic if provided from different actors. Considering the stated results this would be preferred as it enables controls of different kinds. When using a single unit the control strategy has to be considered, but there are other advantages. It could be installed where transmission capacity in the grid is enough to support the power output, it would facilitate potential maintenance, it could be placed strategically and easily accessible, and having a single location might reduce cost of installation.

The potential issues of reduced inertia and increased frequency instability in the Nordic power system have again been demonstrated in this thesis, in a similar manner to what is done in [1], [2], [12], [23], and [49]. But despite this there is currently no mention of kinetic energy or inertia in the Nordic system operation agreement. There is a need to address these issues and one way could be to redefine or even define values of certain limits and parameters used as boundaries of operation. The recommendation is to define, redefine or even just consider: limits of system kinetic energy and inertia, dimensioning fault, frequency nadir, and maximum allowed rate of change of frequency. This is to ensure the issue of reduced inertia has been properly addressed and assure future system stability can be maintained.

8.2 Limits of the Results

The results shown in section 7.2, indicate how BESS can help improve power system frequency stability in the Nordic synchronous power system. These results correlate with theory and findings of similar studies in [12], [23], [49], [59], [63]. But despite this, the results of this thesis should be interpreted with some degree of caution.

The grid model developed in PSS/E and used in this thesis is of a larger scale than what is used in most in comparable studies, but it is still an aggregated model. The choice of using this model was motivated by it being based on open sources, because of it being readily available and for simplicity reasons. Another model could have been used or developed but this would have been time consuming and would perhaps not resulted in eliminating the limits of the model.

The limits of the model and in PSS/E is indicated in section 5.5, where rate of change of frequency (RoCoF) and frequency nadir when reducing inertia was not lowered as much as anticipated. This is thought to be caused by the considerable amount of frequency regulation provided from many generators, but there could be other sources of errors. Most notable is the somewhat extreme simplification made when modeling connection points to other countries where each point is represented by a single unit. Additionally, units of the same type are all assigned the same dynamic PSS/E models and some parameters have been assigned entirely to achieve

the desired dynamic response. Also, several estimations and assumptions are applied, particularly when estimating kinetic energy. These choices were motivated and especially for simplicity reasons and in order to ensure this project could be completed in time.

The production and demand case used in this thesis is a high load case at 10.00-11.00 on 05 March 2015. As mentioned in section 5.2, this case was chosen because there was a reference frequency response for the Nordic synchronous system at 11.04 when Ringhals 4 was disconnected and the dynamic response of the grid model was adjusted to this reference response. Therefore, the results are essentially only valid for this case and the results are used as a general indication of potential benefits of BESS.

The battery storage control models developed in chapter 6, behave as designed and their benefits are presented when implemented in the simulations. The derivative controlled model demonstrates to be better than real inertial response in subsection 7.2.5, but despite this there are limits to these models as well. No frequency filter is applied in either model, which for the grid model used in this thesis was not deemed necessary. The disadvantage of this assumption is shown in subsection 7.2.3, where large derivative controlled units produce major frequency distortion at the local bus. The suggestion is to add a frequency filter, which is done other BESS studies [4], [59], [62], [63]. This might improve the response of the derivative controlled model by reducing the occurrence of sudden power surges. With a filter, it might also be possible implement a derivative control based on the instantaneous change in frequency if true inertial response is desired.

8.3 Sustainable and Ethical Aspects

Sustainable development and ethical outlooks are also important to consider when contemplating battery storage applications in the Swedish power system.

8.3.1 Battery Systems for Power System Applications

In many countries battery systems are increasingly used complementary to renewable energy in order to phase out fossil fueled production. The carbon dioxide emissions are the major sustainable disadvantage of conventional power production with high consumption of fossil fuel. In Sweden and countries with similar production, this is not the case and battery storage is worse in this aspect than conventional power generation.

Large portion of the lithium-ion battery industry is conducted in China and the carbon footprint of this industry is significant [74]. In the transport sector, electric vehicles are a key solution to reducing tail-pipe emissions and air pollution [31]. For these cases, emissions on a global scale caused by the production of lithium-ion batteries can be seen as an inevitable necessity to reduce emissions on a local scale in large cities. But for BESS for power system applications this argument does not

hold.

Large scale lithium-ion factories, such as the Northvolt battery factory, in countries with low or no fossil fueled production are instead seen as enablers in the desired deployment of BESS in power system applications with lower life cycle emissions. By using batteries from these factories, the carbon emission life cycle footprint will be significantly reduced as the energy needed to produce the batteries will come from sustainable and more ethically produced sources. The hope is also that this will stimulate the recycling industry of lithium-ion batteries that today is almost nonexistent [75].

Other sustainable and ethical aspects that should not be overseen when discussing lithium-ion batteries are the working conditions and environmental consequences of obtaining material. Rare earth materials are needed to produce lithium-ion batteries and with increased demand the shortage of crucial materials will not only increase prices but also risk create social issues. Cobalt, lithium and nickel supply chains are sources of ethical concerns and can cause social and political conflicts, human rights abuses, health problems and environmental impacts [76], [77], [78]. With the number of different materials needed to produce a battery it is difficult to ensure the materials are ethically obtained and produced.

The intended use of lithium-ion BESS in power systems applications is also not without potential risks. Because of the high-power density, explosions and fires are a concern, as mentioned in subsection 4.2.5. Lithium-ion fires generate immense heat, but also toxic smoke and gas, and this gas pollution might even be a greater threat than the fire [79].

These aspects of BESS should all be considered and compared against the potential benefits when considering the technology for power system application. However, the alternatives to BESS should also to be considered. One alternative is keeping or even increasing conventional production from nuclear generation as decommission of nuclear power will result in reduced kinetic energy and system inertia. In subsection 7.2.5, it is shown how a 540 MW BESS can be used to substitute the reduction of kinetic energy equivalent to roughly the amount of kinetic energy from twice the installed capacity of nuclear power in Sweden. Nuclear energy is in some aspects regarded as an energy source that can help reduce greenhouse gas emissions and maintain system frequency stability. But on the other hand, the sustainable and ethical disadvantages of nuclear power are well established with highly toxic radioactive waste, irreversible effects on public health and environment and any nuclear disasters have catastrophic global impact [80]. Other technological techniques providing services similar to inertial response and frequency regulation are perhaps a better choice.

In [23] several techniques capable of providing services that can improve the frequency stability are mentioned and suggested. These are wind turbines, HVDC links, flywheels, synchronous condensers, supercapacitors and services such as de-

mand response and vehicle to grid applications. When these technologies are compared to lithium-ion BESS, most (except perhaps vehicle to grid applications) are considered to have lower environmental impact and are more sustainable. They might not be better from a technically but from a sustainable perspective they are preferable.

8.3.2 Ethical Consequences of the Work

The grid model used in this thesis and the generator control models developed for BESS have been based on second hand sources. This was motivated by wanting to ensure all information could be made available and avoid any issues of secrecy or intellectual property rights. One issue related to this is concerned with properly crediting the contribution of others. A great deal of attention has been paid to ensure it is clearly stated what contributions are from others, but there are still minor risks that this has been overlooked in some cases.

Another related issue is being realistic and honest when stating claims, assumptions or estimated based on available data. It is recognized that over relying on certain data can have major impact on following results. This has been considered in this thesis by trying to verify the data and by using several sources of data have whenever possible. This is especially relevant to the grid model contributions, kinetic energy estimations, and BESS control models developed in this thesis.

The limits of this thesis have been declared, potential sources of errors have been pointed out and the results are stated as only being indications of the potential benefit of BESS in frequency control. But there is a risk that certain limits or sources of potential errors of the thesis have not been disclosed properly.

There is no intended attempt to exaggerate the potential benefits of BESS. As mentioned in section 1.1, there are several solutions to the issues of frequency stability and reduced inertia in the power system. This thesis is limited to BESS, but it is just one of many prospective technologies and it is important to consider other solutions to diversify conclusions drawn from this thesis.

9
Conclusion

In this work the possibilities of using battery energy storage systems (BESS) for frequency control in the Nordic power system have been investigated. Based on a comparison of different battery technologies lithium-ion technology was found to be the most suited for the intended purpose to provide inertial response and FCR-D. The main advantages were its high efficiency, power capabilities, and benefits of already being commercialized.

From simulations using BESS in the Swedish transmission grid model it was found that derivative controlled BESS reduced RoCoF and increased time to frequency nadir. Droop controlled BESS were effective in raising frequency nadir and reduced following oscillations.

It was also found that distributing 540 MW power capacity over 11 units instead of using a single unit of 540 MW had major implications on frequency distortion at the local bus when using derivative controlled BESS. For droop controlled BESS it was found to be no difference in using a single large unit of 540 MW or several smaller ones with total capacity of 540 MW. The simulation study using derivative controlled BESS to provide the equivalent to kinetic energy of 130 000 MWs during the frequency event showed that it was successful in providing a support comparable to inertial response by reducing RoCoF. It also slightly improved stability after frequency nadir was reached.

The findings of the economic and lifetime feasibility study were that the cost of a lithium-ion BESS is difficult to cover with the income from the current Nordic FCR-D market. Considering the current definitions of the market services and requirements, and cost and lifetime of the battery system it is currently deemed economically unfeasible to use a lithium-ion BESS in the FCR-D market.

9.1 Future Work

Considering that BESS possess desired characteristics it is recommended to investigate the possibilities of creating incentives, introduce new market services, redefine requirements or look at alternative support functions, to enable the deployment of battery systems for power system applications in Sweden. Another alternative would be to develop and commercialize sodium-sulfur BESS, which have similar performance characteristics at a lower cost.

Using lithium-ion BESS in the market of FCR-N should be investigated. In this study, only the FCR-D market was considered as it was assumed that the high cycling rate required for a BESS to provide FCR-N would severely limit lifetime. However, since the price for FCR-N is higher than for FCR-D more money can be earned from this application, which might make this application profitable despite resulting in shorter lifetime. The droop model developed in this thesis has introduced the dead band frequency limits as variables and therefore it can be adjusted to provide FCR-N as well.

The developed BESS control models can also be used to model other battery technologies. This can be done by varying the control parameters: efficiency, SOC limits, response time, etc. This can be used to study the effects on the Nordic power system when using BESS based on different types of battery technologies.

The grid model used and the models of BESS developed in this thesis have several development opportunities. The modeled system should be complemented with correct wind capacity and equipped with appropriate dynamic wind turbine models and parameters, which could be useful for future dynamic studies and perhaps studies of synthetic inertia from wind turbines. The modeled grid of Sweden is detailed, and in future work it is recommended to also establish the same accuracy for the whole Nordic synchronous system, for Norway, Finland and Denmark.

The BESS models can be improved by creating a filter to expand the applicability of the models in other systems with more frequency variations. If or when relevant requirements are established in the system operation agreement, e.g. limits to RoCoF, these should be considerd in the control. More characteristics of battery systems can also be included in the models, such as voltage control.

Additional production cases should be investigated. A low load case with high wind production and high import through HVDC links is when frequency stability issues related to inertia are deemed to be the greatest [1], [2], [23], mentioned in section 5.5. This case should be prioritized to show how effective BESS are in cases with low frequency stability. It would also be interesting to vary the load conversion factors to investigate different load frequency dependencies. In the future Nordic power system, the number of frequency dependent loads are expected to decrease [1], [2], [12]. This will have negative impact on system frequency during a fault. By varying load conversion factors, load frequency dependence can be decreased and the effects on the power system can be investigated.

It is also recommended to investigate alternative techniques that potentially can deliver services similar to those from BESS, such as inertial response and frequency regulation. Examples of such techniques include wind turbines, HVDC links, flywheels, synchronous condensers, supercapacitors and even services such as demand response and vehicle to grid applications.

Bibliography

[1] Svenska kraftnät, Statnett, Fingrid and Energinet.dk, "Challenges and Opportunities for the Nordic Power System," Oslo, Norway, Aug. 2016. [Online]. Available: https://www.svk.se/contentassets/9e28b79d9c4541bf82f21938bf8c7389/stet0043_nordisk_rapport_hele_mdato1.pdf , Accessed on: Jan 16, 2018.

[2] D. Karlsson, "IVA - Vägval el: "Svängmassans" roll i elsystemet," Gothia Power, Gothenburg, Sweden, U-DKa-15-006-01C, 2015. [Online]. Available: https://www.iva.se/globalassets/rapporter/vagval-el/201606-iva-vagvalel-svangmassa-c.pdf , Accessed on: Jan 16, 2018. [In Swedish]

[3] P. Tielens, D. V. Hertem "The relevance of inertia in power systems," in *Renewable and Sustainable Energy Reviews*, vol. 55, pg. 999-1009, A. M. Foley, Ed. Elsevier Ltd. Mar. 2016. [Online]. Available: https://www.sciencedirect.com/science/article/pii/S136403211501268X , Accessed on: Jan 16, 2018.

[4] V. Knap, *et al.*, "Sizing of an Energy Storage System for Grid Inertial Response and Primary Frequency Reserve," in *IEEE Transactions on Power Systems*, vol. 31, issue: 5, pg. 3447-3456, N. Hatziargyriou, Ed. IEEE Explore. Dec. 2015. [Online]. Available: http://ieeexplore.ieee.org/document/7355404/ , Accessed on: Jan 16, 2018.

[5] C. Zhang, *et al.* "Energy storage system: Current studies on batteries and power condition system," in *Renewable and Sustainable Energy Reviews*, vol. 82, part 3, pg. 3091-3106, A. M. Foley, Ed. Elsevier Ltd. Feb. 2018. [Online]. Available: https://www.sciencedirect.com/science/article/pii/S1364032117314077 , Accessed on: Jan 16, 2018.

[6] "Optimal Provision of Primary Frequency Control with Battery Systems by Exploiting All Degrees of Freedom within Regulation," in *Energy Procedia*, vol. 99, pg. 204-214, J. Yan, Ed. Elsevier Ltd. Nov. 2016. [Online]. Available: https://www.sciencedirect.com/science/article/pii/S1876610216310724 , Accessed on: Jan 19, 2018.

[7] D. M. Greenwood *et al.*, "Frequency response services designed for energy storage," in *Applied Energy*, vol. 203, pg. 115-127, J. Yan, Ed. Elsevier Ltd. Oct. 2017. [Online]. Available: https:

//www.sciencedirect.com/science/article/pii/S0306261917307729 , Accessed on: Jan 16, 2018.
[8] L. Messing and S. Lindahl "Inventering av framtidens el- och värmeproduktionstekniker: Delrapport Energilagring," Elforsk AB, Stockholm, Sweden, Report 08:83, Dec. 2008. [Online]. Available: https://goo.gl/98bCLi , Accessed on: Jan 19, 2018. [In Swedish]
[9] G. J. May, A. Davidson, and B. Monahov, "Lead batteries for utility energy storage: A review," in *Journal of Energy Storage*, vol. 15, D. U. Sauer, Ed. 2018, pp. 145-157. [Online]. Available: https://www.sciencedirect.com/science/article/pii/S2352152X17304437#bib0005 , Accessed on: Feb 02, 2018.
[10] P. Nikolaidisa and A. Poullikkas, "Cost metrics of electrical energy storage technologies in potential power system operations," in *Sustainable Energy Technologies and Assessments*, vol. 25, L. Schaefer, Ed. 2018, pp. 43-59. [Online]. Available: https://www.sciencedirect.com/science/article/pii/S2213138817304563 , Accessed on: Feb 02, 2018.
[11] "DOE Global Energy Storage Database," U.S. Department of Energy, Washington D.C., USA, 2018. [Online]. Available: http://www.energystorageexchange.org/ , Accessed on: Feb 01, 2018.
[12] A. Danell *et al.*, "Nordic Future System Inertia," European Network of Transmission System Operators for Electricity (ENTSO-E), Brussels, Belgium, 2015. [Online]. Available: https://www.entsoe.eu/Documents/Publications/SOC/Nordic/Nordic_report_Future_System_Inertia.pdf , Accessed on: Jan 22, 2018.
[13] P. Kundur, "Introduction to the Power System Stability Problem," in *Power System Stability and Control* N. J. Balu and M. G. Lauby, Ed. New York, USA: McGraw-Hill Inc., 1994, pp. 17-41
[14] "Nordic Balancing Philosophy," European Network of Transmission System Operators for Electricity (ENTSO-E), Brussels, Belgium, 2016. [Online]. Available: https://www.svk.se/contentassets/bc60c82ceaec44c0b9ffbf3ee2126adf/nordic-balancing-philosophy-160616-final_external.pdf , Accessed on: Jan 25, 2018.
[15] P. Kundur, "Synchronous Machines Theory and Modelling," in *Power System Stability and Control* N. J. Balu and M. G. Lauby, Ed. New York, USA: McGraw-Hill Inc., 1994, pp. 128-131
[16] M. Seyedi and M. Bollen (STRI) "The utilization of synthetic inertia from wind farms and its impact on existing speed governors and system performance: Part 2 Report of Vindforsk Project V-369," Elforsk AB, Stockholm, Sweden, Report 13:02, Jan. 2013.
[17] "Slutrapport pilotprojekt Flexibla hushåll," Svenska Kraftnät, Sundbyberg, Sweden, Svk 2016/1688, 2017. [Online]. Available: https://www.svk.se/siteassets/om-oss/rapporter/2017/slutrapport-pilotprojekt-flexibla-hushall.pdf , Accessed on: Jan 25, 2018. [In Swedish]

[18] "System Operation Agreement appendices (English 2017 update)," European Network of Transmission System Operators for Electricity (ENTSO-E), Brussels, Belgium, 2017. [Online]. Available: https://www.entsoe.eu/Documents/Publications/SOC/Nordic/System_Operation_Agreement_appendices_%28English_2017_update%29.pdf , Accessed on: May 07, 2018.

[19] Balance Responsibility Contract/2628, Version 2628-2, Feb 2018. *Avtal om Balansansvar för el mellan Affärsverket svenska kraftnät ("Svenska kraftnät") och "Balansansvarig"*. [Online]. Available: https://www.svk.se/siteassets/aktorsportalen/elmarknad/balansansvar/dokument/balansansvarsavtal/balansansvarsavtal-uppdaterad-version.pdf , Accessed on: May 07, 2018. [In Swedish]

[20] Commission's Regulation (EU) 2016/631, 14 April 2016, *Fastställande av nätföreskrifter med krav för nätanslutning av generatorer*. [Online]. Available: http://eur-lex.europa.eu/legal-content/SV/TXT/PDF/?uri=CELEX:32016R0631&from=SV , Accessed on: Feb 06, 2018. [In Swedish]

[21] "Technical Requirements for Frequency Containment Reserve Provision in the Nordic Synchronous Area," European Network of Transmission System Operators for Electricity (ENTSO-E), Brussels, Belgium, 2017. [Online]. Available: http://www.statnett.no/Global/Dokumenter/Kraftsystemet/Systemansvar/Technical%20Requirements%20for%20Frequency%20Containment%20Reserve%20Provision%20in%20the%20Nordic%20Synchronous%20Area.pdf , Accessed on: May 07, 2018.

[22] "Supporting Document on Technical Requirements for Frequency Containment Reserve Provision in the Nordic Synchronous Area" European Network of Transmission System Operators for Electricity (ENTSO-E), Brussels, Belgium, 2017. [Online]. Available: http://www.statnett.no/Global/Dokumenter/Kraftsystemet/Systemansvar/Supporting%20Document%20on%20Technical%20Requirements%20for%20Frequency%20Containment%20Reserve%20Provision%20in%20the%20Nordic%20Sy.pdf , Accessed on: Feb 01, 2018.

[23] M. Persson, "Frequency Response by Wind Farms in Power Systems with High Wind Power Penetration," Ph.D. dissertation, Department of Electrical Engineering, Chalmers University of Technology, Gothenburg, Sweden, 2017. [Online]. Available: http://publications.lib.chalmers.se/records/fulltext/250313/250313.pdf , Accessed on: Jan 23, 2018.

[24] "Marknader för förbrukningsflexibilitet," (Supporting document for [17]), Svenska Kraftnät, Sundbyberg, Sweden, [Online]. Available: https://www.svk.se/siteassets/aktorsportalen/elmarknad/reserver/var-passar-just-din-flexibilitet-bast_ny.pdf , Accessed on: Jan 25, 2018. [In Swedish]

[25] "DS3 System Services: Portfolio Capability Analysis," EirGrid and SONI, 2014. [Online]. Available: http://www.eirgrid.ie/site-files/library/EirGrid/DS3-System-Services-Portfolio-Capability-Analysis.pdf , Accessed on: Feb 28, 2018.

[26] "Enhanced frequency response (EFR)," National Grid, London, UK, 2018. [Online]. Available: https://www.nationalgrid.com/uk/electricity/balancing-services/frequency-response-services/enhanced-frequency-response-efr , Accessed on: Jan 25, 2018.

[27] P. Kundur, "Control of Active Power and Reactive Power," in *Power System Stability and Control* N. J. Balu and M. G. Lauby, Ed. New York, USA: McGraw-Hill Inc., 1994, pp. 590-596.

[28] M. T. Lawder, *et al.*, "Battery Energy Storage System (BESS) and Battery Management System (BMS) for Grid-Scale Applications," in *Proceedings of the IEEE* 2014. [Online]. Available: https://pdfs.semanticscholar.org/4c38/39b9145a8b528497faaebfabb81bbd042c72.pdf , Accessed on: Feb 01, 2018.

[29] G. Parkinson, "Explainer: What the Tesla big battery can and cannot do," *Renew Economy*, 2017. [Online]. Available: http://reneweconomy.com.au/explainer-what-the-tesla-big-battery-can-and-cannot-do-42387/ , Accessed on: Mar. 26, 2018.

[30] "A Guide to Understanding Battery Specifications" MIT Electric Vehicle Team, Cambridge, Massachusetts, United States, 2008. [Online]. Available: http://web.mit.edu/evt/summary_battery_specifications.pdf , Accessed on: Feb 01, 2018.

[31] E. Wikner, "Lithium ion Battery Aging: Battery Lifetime Testing and Physics-based Modeling for Electric Vehicle Applications," Lic. thesis, Department of Electrical Engineering, Chalmers Univeristy of Technology, Gothenburg, Sweden, 2017. [Online]. Available: http://publications.lib.chalmers.se/records/fulltext/249356/249356.pdf , Accessed on: Mar. 26, 2018.

[32] J. Zhang, C. Chen, X. Zhang and S. Liu, "Study on the Environmental Risk Assessment of Lead-Acid Batteries," in *Procedia Environmental Sciences*, vol. 31, J. Li and F. Dong, Ed. 2016, pp. 873-879. [Online]. Available: https://www.sciencedirect.com/science/article/pii/S1878029616001043 , Accessed on: Feb 02, 2018.

[33] A. Poullikkas, "A comparative overview of large-scale battery systems for electricity storage," in *Renewable and Sustainable Energy Reviews*, vol. 27, A. M. Foley, Ed. 2013, pp. 778-788. [Online]. Available: https://www.sciencedirect.com/science/article/pii/S1364032113004620 , Accessed on: Feb 06, 2018.

[34] R. L. Fares, J. P. Mayers, and M. E. Webber, "A dynamic model-based estimate of the value of a vanadium redox flow battery for frequency regulation in Texas," in *Applied Energy*, vol. 113, J. Yan, Ed. 2014, pp. 189-198. [Online]. Available: https://www.sciencedirect.com/science/article/pii/S0306261913005916 , Accessed on: Feb 02, 2018.

[35] H. Berg, Batteries for Electric Vehicles, Materials and Electrochemistry. Cambridge University Press, AB Libergreen, Sweden, 2015.

[36] H. D. Abruña, Y. Kiya, and J. C. Henderson, "Batteries and electrochemical capacitors," in *Physics Today*, vol. 61, no. 12, pp. 43–47, 2008.
[37] J. Vetter, *et al.*, "Aging mechanism in lithium ion batteries," in *Journal of Power Sources*, vol. 147, no. 1-2, pp. 269-281, 2005.
[38] J. Lindstens, "Study of a battery energy storage system in a weak distribution grid," MSc. thesis, Uppsala University, Uppsala, Sweden, 2017. [Online]. Available: https://uu.diva-portal.org/smash/get/diva2:1112854/FULLTEXT01.pdf, Accessed on: Mar. 26, 2018.
[39] S. Yarlagadda, T. T. Hartley, and I. Husain, " A battery management system using an active charge equalization technique based on a DC/DC converter topology," in *IEEE Transactions on Industry Applications*, vol. 49, issue. 6, T. A. Nondahl, Ed. 2013, pp. 2720-2729. [Online]. Available: https://ieeexplore.ieee.org/document/6519313/, Accessed on: Mar. 26, 2018.
[40] H. Rahimi-Eichi, U. Ojha, F. Baronti, and M. Y. Chow, "Battery management system: an overview of its application in the smart grid and electric vehicles," in *IEEE Industrial Electronics Magazine*, vol. 7, issue. 2, T. Sauter, Ed. 2013, pp. 4-16. [Online]. Available: https://ieeexplore.ieee.org/document/6532486/, Accessed on: Mar. 26, 2018.
[41] R. Kaiser, "Optimized battery-management system to improve storage lifetime in renewable energy systems," in *Journal of Power Sources*, vol. 168, issue. 1, S. Passerini, Ed. 2007, pp. 58–65. [Online]. Available: https://www.sciencedirect.com/science/article/pii/S0378775306025420, Accessed on: Mar. 26, 2018.
[42] S. W. Hwangbo, B. J. Kim, and J. H. Kim, "Application of economic operation strategy on battery energy storage system at Jeju," in *Innovative Smart Grid Technologies Latin America (ISGT LA), 2013 IEEE PES Conference* 2013, pp. 1–8. [Online]. Available: https://ieeexplore.ieee.org/document/6554367/, Accessed on: Mar. 26, 2018.
[43] A. Thorslund, "Swedish Transmission Grid Model Based on Open Sources," MSc thesis, Department of Electrical Engineering, Chalmers University of Technology, Gothenburg, Sweden, 2017.
[44] "Elåret & Verksamhetsåret 2015," Swedenergy, Stockholm, Sweden, 2016 [Online]. Available: http://www.svenskenergi.se/Global/Statistik/El%C3%A5ret/el%C3%A5ret2015_160429_web2.pdf , Accessed on: Feb 28, 2018. [In Swedish]
[45] S. Arnborg, "Reaktivt effektutbyte," Svenska Kraftnät, Sundbyberg, Sweden, [Online]. Available: https://www.svk.se/siteassets/om-oss/organisation/vara-rad/planeringsradet/arkiverat/bilaga-1-reaktivt-effektutbyte.pdf , Accessed on: Feb 28, 2018. [In Swedish]
[46] "Historical Market Data," Nord Pool Group, Lysaker, Norway, 2018. [Online]. Available: https://www.nordpoolgroup.com/historical-market-data/ , Accessed on: Mar 05, 2018.

[47] "ENTSO-E Transmission System Map," European Network of Transmission System Operators for Electricity (ENTSO-E), 2017. [Online]. Available: https://www.entsoe.eu/map/Pages/default.aspx , Accessed on: Feb 28, 2018.
[48] G. Jancke and R. Engström, *Elektriska data för högspända kraftledningar*. AB Svenska Metallverken, 1955. [In Swedish]
[49] S. M. Hamre, "Inertia and FCR in the Present and Future Nordic Power System - Inertia Compensation," MSc thesis, Department of Electric Power Engineering, Norwegian University of Science and Technology, Trondheim, Norway, 2015. [Online]. Available: https://brage.bibsys.no/xmlui/handle/11250/2368231 , Accessed on: Mar 05, 2018.
[50] L. Vanfretti *et al.*, "An open data repository and a data processing software toolset of an equivalent Nordic grid model matched to historical electricity market data," in *Data in Brief*, vol. 11, pg. 349-357, H. R. Wang and G. Lan, Ed. Apr. 2017, [Online]. Available: https://www.sciencedirect.com/science/article/pii/S2352340917300409 , Accessed on: Mar 05, 2018.
[51] L. Vanfretti *et al.*, "iTesla Power Systems Library (iPSL): A Modelica library for phasor time-domain simulations," in *SoftwareX*, vol. 5, pg. 84-88, Dr. K. Keahey *et al.*, Ed. 2016 [Online]. Available: https://www.sciencedirect.com/science/article/pii/S2352711016300097?via%3Dihub , Accessed on: Mar 05, 2018.
[52] *PSS/E 34.2 Model Library*, Siemens Industry Inc. Siemens Power Technologies International, Schenectady, NY USA, 2017.
[53] *PSS/E 34.2 Program Application Guide Vol. 1*. Siemens Industry Inc. Siemens Power Technologies International, Schenectady, NY, USA, 2017.
[54] S. Persic, "Frekvensreglering i det nordiska kraftsystemet: Modellering i PSS/E," MSc thesis, Department of Electrical and System Engineering, KTH Royal Institute of Technology, Stockholm, Sweden, 2007. [Online]. Available: https://www.svk.se/siteassets/jobba-har/dokument/exjobb2007_frekvensreglering.pdf , Accessed on: Mar 05, 2018. [In Swedish]
[55] "Underlagsrapport – Överföring," Svenska Kraftnät, Sundbyberg, Sweden, 2015. [Online]. Available: http://www.sou.gov.se/wp-content/uploads/2017/01/Underlagsrapport_Svenska-Kraftn%C3%A4t_%C3%96verf%C3%B6ring.pdf , Accessed on: Mar 05, 2018. [In Swedish]
[56] PSS/E 34.2 Program Application Guide Vol. 2 Siemens Industry Inc. Siemens Power Technologies International, Schenectady, NY, USA, 2017.
[57] J. Djurström and J. Ulleryd, "Ny frekvensregulatormodell för simuleringsprogrammet PSS/E," MSc thesis, Department of Electric Power Systems Chalmers University of Technology, Gothenburg, Sweden, 1994. [In Swedish]
[58] "System Impact Assessment Report Connection Assessment & Approval Process," IESO, Ontario, Canada, 2010. [Online]. Available:

www.ieso.ca/-/media/Files/IESO/caa/CAA_2007-294_Final_Report.pdf , Accessed on: Mar 05, 2018.

[59] O. J. Moreno, "Ancillary Service for Frequency Support Design of a Battery Storage Based Ancillary Service for Frequency Support in the Nordic Power System," MSc. thesis, Department of Electrical Engineering, Chalmers University of Technology, Gothenburg, Sweden, 2017. [Online]. Available: http://publications.lib.chalmers.se/records/fulltext/252399/252399.pdf, Accessed on: Apr. 29, 2018.

[60] D. Doheny "Investigation into the Local Nature of Change of Frequency in Electrical Power Systems," in *Student Journal of Energy Research*, vol. 2, no. 1, article 3, Dublin Institute of Technology, 2017. [Online]. Available: https://arrow.dit.ie/cgi/viewcontent.cgi?referer=https://www.google.se/&httpsredir=1&article=1003&context=sjer, Accessed on: Apr. 14, 2018.

[61] X. Xu, M. Bishop, D. G. Oikarinen, and C. Hao, "Application and Modeling of Battery Energy Storage in Power Systems," in *CSEE Journal of Energy and Power Systems*, vol. 2, no. 3, 2016, pp. 82-90. [Online]. Available: http://ieeexplore.ieee.org/stamp/stamp.jsp?arnumber=7562828, Accessed on: Mar. 26, 2018.

[62] M. C. Such, "Operation and Control Strategies for Battery Energy Storage Systems to Increase Penetration Levels of Renewable Generation of Remote Microgrids," MSc. thesis, The University of Texas, Austin, Texas, USA, 2013 [Online]. Available: https://repositories.lib.utexas.edu/bitstream/handle/2152/22271/SUCH-THESIS-2013.pdf?sequence=1, Accessed on: Mar. 26, 2018.

[63] D. H. Son and S. R. Nam, "Development of PSS/E Dynamic Model for Controlling Battery Output to Improve Frequency Stability in Power Systems," in *International Journal of Energy and Power Engineering*, vol. 11, no. 4, 2017, pp. 462-466. [Online]. Available: https://goo.gl/JLmvEW, Accessed on: Mar. 26, 2018.

[64] G. M. Gloria, C. Gueifao, and J. F. de Jesus, "Battery Energy Storage System in a 100% renewable network: Case study of Brava Island," Department of Energy, Universidade de Lisboa, Lisbon, Portugal, 2017. [Online]. Available: http://gestoenergy.com/wp-content/uploads/2017/01/BravaPaper.pdf, Accessed on: Mar. 26, 2018.

[65] *PSS/E 34.2 Program Operation Manual* Siemens Industry Inc. Siemens Power Technologies International, Schenectady, NY, USA, 2017.

[66] X. Luo, J. Wang, M. Dooner, and J. Clarke "Overview of current development in electrical energy storage technologies and the application potential in power system operation," in *Applied Energy*, vol. 137, issue. 1, J. Yan, Ed. 2015, pp. 511-536. [Online]. Available: https://www.sciencedirect.com/science/article/pii/S0306261914010290, Accessed on: Apr. 04, 2018.

[67] C. Bordin, *et al.*, "A linear programming approach for battery degradation analysis and optimization in offgrid power systems with solar energy integration," in *Renewable Energy*, vol. 101, S. Kalogirou, Ed. 2017, pp.

417-430. [Online]. Available: https://www.sciencedirect.com/science/article/pii/S0960148116307765, Accessed on: Apr. 19, 2018.

[68] S. B. Peterson, J. F. Whitacre, and J. Apt, "The economics of using plug-in hybrid electric vehicle battery packs for grid storage," in *Journal of Power Sources*, vol. 195, issue. 8, S. Passerini, Ed. 2010, pp. 2377-2384. [Online]. Available: https://www.sciencedirect.com/science/article/pii/S0378775309017303, Accessed on: Apr. 19, 2018.

[69] R. Dufo-Lopez, J. L.Bernal-Agustín, and J. A. Domínguez-Navarro, "Generation management using batteries in wind farms: Economical and technical analysis for Spain," in *Energy Policy*, vol. 37, issue. 1, S. P. A. Brown and M. Jefferson, Ed. 2009, pp. 126-139. [Online]. Available: https://www.sciencedirect.com/science/article/pii/S0301421508004138, Accessed on: Apr. 19, 2018.

[70] F.M. Gatta, A. Geri, S. Lauria, M. Maccioni, and F. Palone, "Battery energy storage efficiency calculation including auxiliary losses: Technology comparison and operating strategies," in *PowerTech, 2015 IEEE Eindhoven*, 2015, [Online]. Available: https://ieeexplore.ieee.org/document/7232464/, Accessed on: Apr. 19, 2018.

[71] "MIMER: Struktur och avräkningsdata för elmarknadens aktörer," Svenska Kraftnät, Sunbyberg, Sweden, 2018. [Online]. Available: https://mimer.svk.se/PrimaryRegulation/PrimaryRegulationIndex, Accessed on: May. 01, 2018. [In Swedish]

[72] "Marknader för förbrukningsflexibilitet – handel och prissättning," Svenska Kraftnät, Sunbyberg, Sweden, 2018. [Online]. Available: https://www.svk.se/siteassets/aktorsportalen/elmarknad/reserver/handel-och-prissattning_ny.pdf, Accessed on: May. 01, 2018. [In Swedish]

[73] Y. Cui, *et al.*, "Multi-stress factor model for cycle lifetime prediction of lithium ion batteries with shallow-depth discharge," in *Journal of Power Sources*, vol. 279, S. Passerini, Ed. 2015, pp. 123-132. [Online]. Available: https://www.sciencedirect.com/science/article/pii/S037877531500004X, Accessed on: May. 02, 2018.

[74] C. Wong, B. Chen, Y. Yu, Y. Wang, and W. Zhang, "Carbon footprint analysis of lithium ion secondary battery industry: two case studies from China," in *Journal of Cleaner Production*, vol. 163, J. J. Klemes, *et al.*, Ed. 2017, pp. 241-251. [Online]. Available: https://www.sciencedirect.com/science/article/pii/S0959652616002341, Accessed on: May. 06, 2018.

[75] L. Gaines, "The future of automotive lithium-ion battery recycling: Charting a sustainable course," in *Sustainable Materials and Technologies*, vol. 1-2, L. Espinal, L. Gaines, A. Ku, and Z. Sun, Ed. 2014, pp. 2-7. [Online]. Available: https:

//www.sciencedirect.com/science/article/pii/S2214993714000037, Accessed on: May. 06, 2018.

[76] L. Hancock, N. Raplh, M. Armand, D. Macfarlane, and M. Forsyth, "In the lab: New ethical and supply chain protocols for battery and solar alternative energy laboratory research policy and practice," in *Journal of Cleaner Production*, vol. 187, J. J. Klemes, *et al.*, Ed. 2018, pp. 485-495. [Online]. Available: https://www.sciencedirect.com/science/article/pii/S0959652618307546, Accessed on: May. 06, 2018.

[77] A. Pehlken, S. Albach, and T. Vogt, "Is there a resource constraint related to lithium ion batteries in cars?," in *The International Journal of Life Cycle Assessment*, vol. 22, issue. 1, M. A. Curran, Ed. 2017, pp. 40-53. [Online]. Available: https://link-springer-com.proxy.lib.chalmers.se/article/10.1007%2Fs11367-015-0925-4, Accessed on: May. 06, 2018.

[78] M. Opray, "Nickel mining: the hidden environmental cost of electric cars," in *The Guradian*, 28 Aug 2017, [Online]. Available: https://www.theguardian.com/sustainable-business/2017/aug/24/nickel-mining-hidden-environmental-cost-electric-cars-batteries, Accessed on: May. 06, 2018.

[79] F. Larsson, P. Andersson, P. Blomqvist, and B. E. Mellander, "Toxic fluoride gas emissions from lithium-ion battery fires," 2017; 7: 10018, 2017. [Online]. Available: https://www.ncbi.nlm.nih.gov/pmc/articles/PMC5577247/, Accessed on: May. 06, 2018.

[80] H. Xiang and Y. Zhu, "The Ethics Issues of Nuclear Energy: Hard Lessons Learned from Chernobyl and Fukushima," in *Online Journal of Health Ethics*, vol. 7, issue. 2, article. 6, Chengdu No. 1 People's Hospital, Chengdu, Sichuan, China, 2011. [Online]. Available: https://aquila.usm.edu/cgi/viewcontent.cgi?article=1099&context=ojhe, Accessed on: May. 06, 2018.

[81] "IEEE Policies 2018," The Institute of Electrical and Electronics Engineers, New York, NY, USA, 2018. [Online]. Available: https://www.ieee.org/content/dam/ieee-org/ieee/web/org/about/whatis/ieee-policies.pdf, Accessed on: May. 06, 2018.